UNIVERSITÀ
DEGLI STUDI
FIRENZE

Scuola di Ingegneria

Corso di Laurea in

Ingegneria Informatica

Optimization methods for Recurrent Neural Networks training

Tesi di Laurea di

Giulio Galvan

Relatori:

Prof. Luís Nunes Vicente
Prof. Marco Sciandrone

Correlatori:

Prof. Fabio Schoen

Anno Accademico 2014/2015

Abstract

In this thesis we introduce the Recurrent Neural Network (RNN) model starting from the more common Feed Forward Neural Networks showing how to use such models to define optimization problems for machine learning. We pay particular attention to the gradient structure of such models because it helps explaining the "infamous" *exploding/vanishing* gradient problem which constitutes the most important difficulty in training RNNs. We show how this problem affects the learning process and we review the solutions that have been developed over time. We then introduce a novel approach based on stochastic gradient descent which deals with the *exploding/vanishing* gradient problem through a careful initialization and by using a descent direction different from the usual anti-gradient. Finally we evaluate our approach both on synthetic and real datasets.

Contents

Chapter 1

Artificial neural networks

1.1 A family of models

An artificial neural network is a network of connected units called neurons or perceptrons, as can be seen in Figure 1.1. The link which connects neurons i and j, is associated with a weight w_{ji}. Perceptrons share the same structure for all models, what really distinguish a particular model, in the family of artificial neural networks, is how the perceptron units are arranged and connected together, for example whether there are cycles or not, and how data inputs are *fed* to the network.

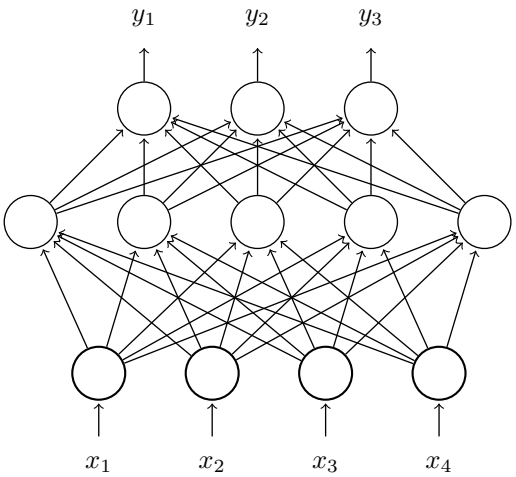

Figure 1.1: Artificial neural network example.

As you can see in Figure 1.2 each neuron is *fed* with a set of inputs which are the weighted outputs of other neurons and/or other external inputs. Formally the output of a perceptron ϕ_j is defined as:

$$\phi_j \triangleq \sigma(a_j) \tag{1.1}$$

$$a_j \triangleq \sum_l w_{jl}\phi_l + b_j \tag{1.2}$$

where w_{jl} is the weight of the connection between neuron l and neuron j, $\sigma(\cdot)$ is some non linear function and $b_j \in \mathbb{R}$ is a bias term. It's worth noticing that in this formulation the inputs ϕ_l can be the outputs of other neurons or provided external inputs.

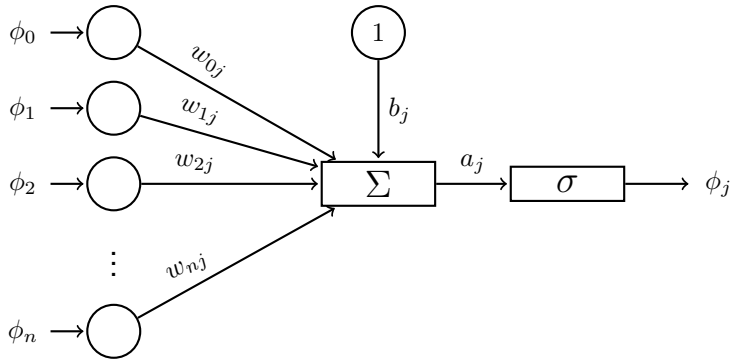

Figure 1.2: Neuron model.

So, given a set of inputs $\{x\}_i$ which are *fed* to some of the units of the net which we call *input units* the output of the network $\{y\}_i$ is given by the some of units of the network, the "upper" ones, which we call *output units*. All remaining units, i.e. the ones which are neither input nor output units are called *hidden units* because their value is not *observed* from the outside.

The activation function The $\sigma(\cdot)$ function is called *activation function* and should determine whether a perceptron unit is *active* or not. When artificial neural networks where first conceived, trying to mimic the brain structure, such function was a simple threshold function, trying to reproduce the behavior of brain neurons: a neuron is *active*, i.e. it's output ϕ_j is 1, if the sum of the input stimuli $\sum_l w_{jl}\phi_l + b_j$ is greater than a given threshold τ.

$$\sigma_\tau(x) = \begin{cases} 1 & \text{if } x > \tau, \\ 0 & \text{otherwise.} \end{cases} \tag{1.3}$$

Such function, however, is problematic when we are to compute gradients because it is not continuous, so one of the following function is usually chosen:

$$sigmoid(x) = \frac{1}{1 + e^{-x}}, \tag{1.4}$$

$$tanh(x) = \frac{e^x - e^{-x}}{e^x + e^{-x}}. \tag{1.5}$$

These functions behave similarly to the threshold function, but, because of their *smoothness*, present no problems in computing gradients. Another function which is becoming a very popular choice is the *rectified linear unit*:

$$ReLU(x) = \begin{cases} x & \text{if } x > 0, \\ 0 & \text{otherwise.} \end{cases} \tag{1.6}$$

ReLU activation function is rather different from previous activation functions, some of these difference, in particular with respect to gradients will be analyzed in later sections.

It is worth noticing that the activation function it is the only component which make artificial neuron networks a non linear model. Were we to choose a *linear* function as activation function we will end up with a simple linear model since the outputs of the network would be ultimately composed only of sums of products.

The bias term Let's consider the old threshold function σ_τ, and ask ourselves what the bias term is for, what does changing this term bring about. Suppose neuron j has no bias term, the neuron value would be $a_j = \sum_l w_{jl}\phi_l$; if $a_j > \tau$ that neuron is active otherwise it is not. Now, let's add the bias term to a_j; we obtain that neuron j is active if $a_j > \tau - b_j$. So the effect of the bias term is to change the activation threshold of a given neuron. Using bias terms in a neural network architecture gives us the ability to change the activation threshold for each neuron; that's particularly important considering that we can learn such

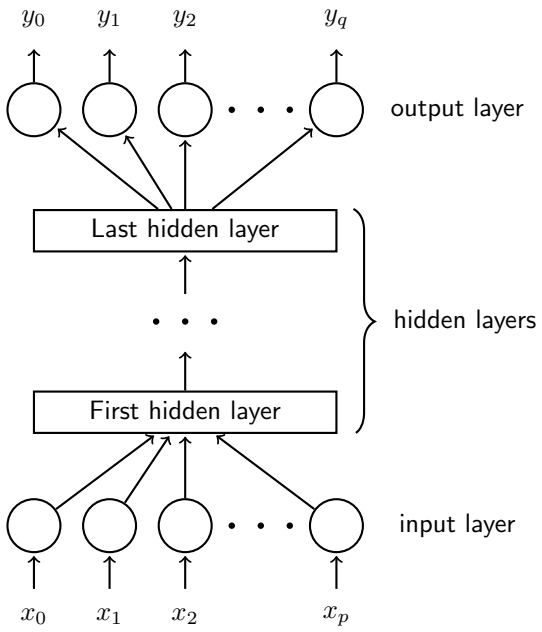

Figure 1.3: Layered structure of an artificial neural network.

bias terms. We can do these same considerations in an analogous way for all the other activation functions.

Layered view of the net It is often useful to think of a neural network as series of layers, one on top of each other, as depicted in Figure 1.3. The first layer is called the *input layer* and its units are *fed* with external inputs, the upper layers are called *hidden layers* because theirs outputs are not observed from outside except the last one, which is called *output layer*, because it's output is the output of the net.

When we describe a network in this way is also useful to adopt a different notation: we describe the weights of the net with a set of matrices W^k one for each layer, and neurons are no more globally indexed, instead with refer to a neuron with a relative index with respect to the layer; this allows to write easier equations in matrix notation [1]. In this notation W^k_{ij} is the weight of the link connecting neuron j of layer k to neuron i of level $k+1$

[1] In the rest of the book we will refer to the latter notation as *layer notation* and to the previous one as *global notation*.

1.2 Feed forward neural networks

A feed forward neural network is an artificial neural network in which there are no cycles, that is to say each layer output is *fed* to the next one and connections to earlier layers are not possible.

Definition 1 (Feed forward neural network)**.** A feed forward neural network is a tuple:

$$\text{FFNN} \triangleq \langle \boldsymbol{p}, \mathcal{W}, \mathcal{B}, \sigma(\cdot), F(\cdot) \rangle.$$

- $\boldsymbol{p} \in \mathbb{N}^U$ is the vector whose elements $p(k)$ are the number of neurons of layer k; U is the number of layers.
- $\mathcal{W} \triangleq \{W^k_{p(k+1)\times p(k)}, k = 1, ..., U-1\}$ is the set of weight matrices of each layer.
- $\mathcal{B} \triangleq \{\boldsymbol{b}^k \in \mathbb{R}^{p(k)}, k = 1, ..., U\}$ is the set of bias vectors.
- $\sigma(\cdot) : \mathbb{R} \to \mathbb{R}$ is the activation function.
- $F(\cdot) : \mathbb{R}^{p(U)} \to \mathbb{R}^{p(U)}$ is the output function.

Remark 1. Given a FFNN:

- The number of output units is $p(U)$.
- The number of input units is $p(1)$.
- The total number of weights is $\mathcal{N}(\mathcal{W}) \triangleq \sum_{k=1}^{U-1} p(k+1)p(k)$.
- The total number of biases is $\mathcal{N}(\mathcal{B}) \triangleq \sum_{k=2}^{U} p(k)$.

Definition 2 (Output of a FFNN)**.** Given a FFNN and an input vector $\boldsymbol{x} \in \mathbb{R}^{p(1)}$ the output of the net $\boldsymbol{y} \in \mathbb{R}^{p(U)}$ is defined by the following:

$$\boldsymbol{y} = F(\boldsymbol{a}^U) \tag{1.7}$$

$$\boldsymbol{h}^i \triangleq \sigma(\boldsymbol{a}^i), \qquad i = 2, ..., U \tag{1.8}$$

$$\boldsymbol{a}^i \triangleq W^{i-1} \cdot \boldsymbol{h}^{i-1} + \boldsymbol{b}^i \qquad i = 2, ..., U \tag{1.9}$$

$$\boldsymbol{h}^1 \triangleq \boldsymbol{x} \tag{1.10}$$

1.2.1 Learning with FFNNs

A widespread application of neural networks is that of machine learning. In the following we will model an optimization problem which rely on FFNNs. To model an optimization problem we first need to define a dataset D as

$$D \triangleq \{\overline{\boldsymbol{x}}^{(i)} \in \mathbb{R}^p, \overline{\boldsymbol{y}}^{(i)} \in \mathbb{R}^q, i = 1, ..., N\} \tag{1.11}$$

The dataset D is composed of N training examples $\overline{\boldsymbol{x}}^{(i)}$, each one of them paired with a label $\overline{\boldsymbol{y}}^{(i)}$.

Then we need a loss function $L_D : \mathbb{R}^{\mathcal{N}(\mathcal{W})+\mathcal{N}(\mathcal{B})} \to \mathbb{R}_{\geq 0}$ over D defined as

$$L_D(\mathcal{W}, \mathcal{B}) \triangleq \frac{1}{N} \sum_{i=1}^{N} L(\overline{\boldsymbol{y}}^{(i)}, \boldsymbol{y}^{(i)}(\mathcal{W}, \mathcal{B})), \tag{1.12}$$

where $L(\overline{\boldsymbol{y}}, \boldsymbol{y}) : \mathbb{R}^{p(U)} \times \mathbb{R}^{p(U)} \to \mathbb{R}$ is an arbitrary loss function computed on the i^{th} example. Note that $\boldsymbol{y}$ is the output of the network, so it depends on $\mathcal{W}$ and $\mathcal{B}$ whether $\overline{\boldsymbol{y}}$ is fixed within the dataset.

The problem is then to find a FFNN which minimize L_D. As we have seen feed forward neural networks allow for large customization: the only variables in the optimization problem are the weights and the biases, the other parameters are called *hyper-parameters* and are determined *a priori*. Usually the output function is chosen depending on what we are trying to learn, for instance for k-way classification is generally used the *softmax* function

$$softmax(x)_i \triangleq \frac{e^{\boldsymbol{x}_i}}{\sum_{j=1}^{k} e^{\boldsymbol{x}_j}}, \tag{1.13}$$

for regression a simple identity function. For what concerns the number of layers and the number of units per layers they are chosen relying on experience or performing some kind of hyper-parameter tuning, which usually consists on training nets with different configurations of such parameters and choosing the 'best one'.

Once we have selected the values for all hyper-parameters the optimization problem becomes:

$$\min_{\mathcal{W},\mathcal{B}} L_D(\mathcal{W},\mathcal{B}) \tag{1.14}$$

1.2.2 Gradient

Consider a FFNN $= \langle \boldsymbol{p}, \mathcal{W}, \mathcal{B}, \sigma(\cdot), F(\cdot)\rangle$, let $L : \mathbb{R}^{p(U)} \times \mathbb{R}^{p(U)} \to \mathbb{R}$ a loss function and $g(\cdot) : \mathbb{R}^{\mathcal{N}(\mathcal{W})+\mathcal{N}(\mathcal{B})} \to \mathbb{R}$ be the function defined by

$$g(\mathcal{W},\mathcal{B}) \triangleq L(F(a^U(\overline{\boldsymbol{y}}^{(i)})), \boldsymbol{y}^{(i)}(\mathcal{W},\mathcal{B})). \tag{1.15}$$

Equation (1.15), tough it seems rather scary, express a very simple thing: we consider a single input example $\overline{\boldsymbol{x}}^{(i)}$, we run it through the network and we confront it's output $F(a^U(\overline{\boldsymbol{x}}^{(i)})$ with it's label $\overline{\boldsymbol{y}}^{(i)}$ using the loss function L; the function $g(\mathcal{W},\mathcal{B})$ it's simply the loss function computed on the i^{th} example which of course depends only on the weights and biases of network since the training examples are fixed within the dataset. In the following we will derive an expression for gradient with respect to a weight matrix W^i and a bias vector $\boldsymbol{b}^i$. Before reading further consider taking a look at the notation appendix.

$$\frac{\partial g}{\partial W^i} = \nabla L^T \cdot J(F) \cdot \frac{\partial \boldsymbol{y}}{\partial \boldsymbol{a}^U} \cdot \frac{\partial \boldsymbol{a}^U}{\partial W^i} \tag{1.16}$$

$$= \frac{\partial g}{\partial \boldsymbol{a}^U} \cdot \frac{\partial \boldsymbol{a}^U}{\partial W^i}. \tag{1.17}$$

To help clarify the notation we provide just for equation 1.16 the dimensions of the matrices involved in the product:

$$[1 \times p(i+1) \cdot p(i)] = [p(U) \times 1] \cdot [p(U) \times p(U)] \cdot [p(U) \times p(i+1) \cdot p(i)].$$

We can easily compute the gradient of L, ∇L, and the jacobian of F, $J(F)$, once we define $F(\cdot)$ and $L(\cdot)$. Note that the weights are not involved in such computation. Let us derive an expression for $\frac{\partial \boldsymbol{a}^U}{\partial W^i}$. We will start deriving such derivative using the global notation. Consider a single output unit u and a weight w_{lj} linking neuron j to neuron l.

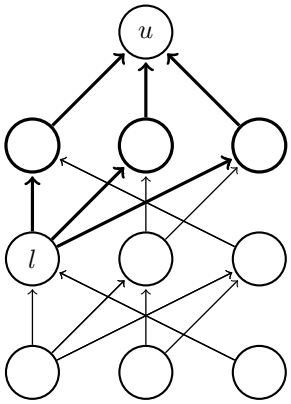

Figure 1.4: Nodes and edges involved in $\frac{\partial a_u}{\partial a_l}$.

$$\frac{\partial a_u}{\partial w_{lj}} = \frac{\partial a_u}{\partial a_l} \cdot \frac{\partial a_l}{\partial w_{lj}} \tag{1.18}$$

$$= \delta_{ul} \cdot h_j, \tag{1.19}$$

where we put

$$\delta_{ul} \triangleq \frac{\partial a_u}{\partial a_l}.$$

Let $P(l)$ be the set of parents of neuron l, formally:

$$P(l) = \{k : \exists \text{ a link between } l \text{ and } k \text{ with weight } w_{lk}\}. \tag{1.20}$$

We can compute δ_{ul} simply applying the chain rule, if we write it down in bottom-up style, as can be seen in Figure 1.4, we obtain:

$$\delta_{ul} = \sum_{k \in P(l)} \delta_{uk} \cdot \sigma'(a_k) \cdot w_{kl}. \tag{1.21}$$

The derivatives with respect to biases are computed in the same way:

$$\frac{\partial a_u}{\partial b_l} = \frac{\partial a_u}{\partial a_l} \cdot \frac{\partial a_l}{\partial b_l} \tag{1.22}$$

$$= \delta_{ul} \cdot 1. \tag{1.23}$$

In layered notation we can rewrite the previous equations as:

$$\frac{\partial a^U}{\partial W^i} = \frac{\partial a^U}{\partial a^{i+1}} \cdot \frac{\partial^+ a^{i+1}}{\partial W^i}, \tag{1.24}$$

$$\frac{\partial^+ a^{i+1}}{\partial W^i_j} = \begin{bmatrix} h^i_j & 0 & \cdots & \cdots & 0 \\ 0 & h^i_j & \cdots & \cdots & 0 \\ \vdots & \vdots & \ddots & \vdots & \vdots \\ 0 & \cdots & \cdots & \cdots & h^i_j \end{bmatrix}, \tag{1.25}$$

$$\frac{\partial a^U}{\partial a^i} \triangleq \Delta^i = \begin{cases} \Delta^{i+1} \cdot diag(\sigma'(\boldsymbol{a}^{i+1})) \cdot W^i & \text{if } i < U, \\ Id & \text{if } i == U, \\ 0 & \text{otherwise,} \end{cases} \tag{1.26}$$

where

$$diag(\sigma'(\boldsymbol{a}^i)) = \begin{bmatrix} \sigma'(a^i_1) & 0 & \cdots & \cdots & 0 \\ 0 & \sigma'(a^i_2) & \cdots & \cdots & 0 \\ \vdots & \vdots & \ddots & \vdots & \vdots \\ 0 & \cdots & \cdots & \cdots & \sigma'(a^i_{p(i)}) \end{bmatrix}. \tag{1.27}$$

The derivatives w.r.t the biases are instead:

$$\frac{\partial a^U}{\partial b^i} = \frac{\partial a^U}{\partial a^i} \cdot \frac{\partial a^i}{\partial b^i} \tag{1.28}$$

$$= \Delta^i \cdot Id. \tag{1.29}$$

Backpropagation. Previous equations are the core of the famous *back-propagation* algorithm which was first introduced by Rumelhart et al. [27]. The algorithm consists in two *passes*, a *forward pass* and a *backward pass* which give the name to the algorithm. The *forward pass* start from the first layer, compute the hidden units values and the proceed to upper layers using the value of the hidden units $\boldsymbol{a^i}$ of previous layers which have already been computed. The *backward pass* instead, start from the topmost layer and computes Δ^i which can be computed, as we can see from equation 1.26 , once it is known Δ^{i+1}, which has been computed in the previous step, and $\boldsymbol{a^i}$ which has been computed in the *forward pass*.

Backpropagation algorithm has time complexity $\mathcal{O}(\mathcal{N}(\mathcal{W}))$.

1.3 Recurrent neural networks

Recurrent neural networks differ from feed forward neural networks because of the presence of recurrent connections: at least one perceptron output at a given layer i is *fed* to another perceptron at a level $j < i$, as can be seen in Figure 1.5. This is a key difference, as we will see in later sections, because it introduces *memory* in the network, changing, somehow, the expressivenessof the model.

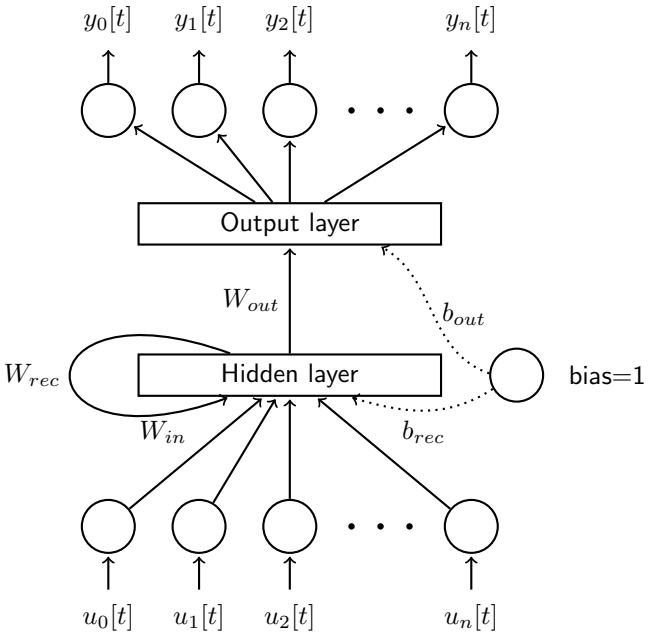

Figure 1.5: RNN model.

This difference in topology reflects also on the network's input and output domain: where, in feed forward neural networks, inputs and outputs were real valued vectors, recurrent neural networks deal with sequences of vectors; in other words time is also considered. One may argue that, taking time (and sequences) into consideration, is some sort of a limitation, because it restricts our model to deal only with temporal inputs; however that is not the case, in fact we can apply RNNs to non temporal data by considering space as the temporal dimension, for example imagine feeding the network with the pixels

of an image one column at a time; or we can feed the network with the same input for all time steps or simply providing no input at all after the first one.

Definition 3 (Recurrent neural network)**.** A recurrent neural network is tuple

$$\text{RNN} \triangleq \langle \mathcal{W}, \mathcal{B}, \sigma(\cdot), F(\cdot) \rangle$$

- $\mathcal{W} \triangleq \{W^{in}, W^{rec}, W^{out}\}$ where
  - W^{in} is the $r \times p$ input weight matrix,
  - W^{rec} is the $r \times r$ recurrent weight matrix,
  - W^{out} is the $o \times r$ output weight matrix.
- $\mathcal{B} \triangleq \{\boldsymbol{b^{rec}}, \boldsymbol{b^{out}}\}$ where
  - $\boldsymbol{b}^{rec} \in \mathbb{R}^r$ is the bias vector for the recurrent layer,
  - $\boldsymbol{b}^{out} \in \mathbb{R}^o$ is the bias vector for the output layer.
- $\sigma(\cdot) : \mathbb{R} \to \mathbb{R}$ is the activation function.
- $F(\cdot) : \mathbb{R}^o \to \mathbb{R}^o$ is the output function.

Remark 2. Given a RNN

- The total number of weights is given by $\mathcal{N}(W) \triangleq rp + r^2 + ro$.
- The number of biases by $\mathcal{N}(b) \triangleq r + o$.
- p is the size of input vectors.
- r is the number of hidden units.
- o is the size of output vectors.

Definition 4 (Output of a RNN)**.** Given a RNN and an input sequence $\{\boldsymbol{x}\}_{t=1,\ldots,T}$, with $\boldsymbol{x}_t \in \mathbb{R}^p$, the output sequence of the net $\{\boldsymbol{y}\}_{t=1,\ldots,T}$, with $\boldsymbol{y}_t \in \mathbb{R}^o$, is de-

fined by the following:

$$\boldsymbol{y}^t \triangleq F(\boldsymbol{z}^t) \tag{1.30}$$

$$\boldsymbol{z}^t \triangleq W^{out} \cdot \boldsymbol{a}^t + \boldsymbol{b}^{out} \tag{1.31}$$

$$\boldsymbol{a}^t \triangleq W^{rec} \cdot \boldsymbol{h}^{t-1} + W^{in} \cdot \boldsymbol{x}^t + \boldsymbol{b}^{rec} \tag{1.32}$$

$$\boldsymbol{h}^t \triangleq \sigma(\boldsymbol{a}^t) \tag{1.33}$$

$$\boldsymbol{h}^0 \triangleq \overrightarrow{0}. \tag{1.34}$$

As we can understand from definition 4, there is only one recurrent layer, whose weights are the same for each time step, so one could asks where does the deepness of the network come from. The answer lies in the temporal unfolding of the network. In fact if we unfold the network step by step we obtain a structure similar to that of a feed forward neural network. As we can observe in Figure 1.6, the unfolding of the network through time consist of putting identical version of the same recurrent layer one on top of each other and linking the inputs of one layer to the next one. The key difference from feed forward neural networks is, as we have already observed, that the weights in each layer are identical; another important unlikeness is of course the presence of additional timed inputs for each unfolded layer.

1.3.1 Learning with RNNs

We can model an optimization problem in the same way we did for feed forward neural networks, the main difference is, again, that we now deal with temporal sequences, so we need a slightly different loss function. Given a dataset D:

$$D \triangleq \{\{\overline{\boldsymbol{x}}^{(i)}\}_{t=1,...,T}, \overline{\boldsymbol{x}}_t^{(i)} \in \mathbb{R}^p, \{\overline{\boldsymbol{y}}^{(i)}\}_{t=1,...,T}, \overline{\boldsymbol{y}}_t^{(i)} \in \mathbb{R}^o; i = 1, ..., N\} \tag{1.35}$$

we define a loss function $L_D : \mathbb{R}^{\mathcal{N}(W)+\mathcal{N}(B)} \to \mathbb{R}_{\geq 0}$ over D as

$$L_D(\mathcal{W}, \mathcal{B}) \triangleq \frac{1}{N} \sum_{i=1}^{N} \sum_{t=1}^{T} L_t(\overline{\boldsymbol{y}}_t^{(i)}, \boldsymbol{y}_t^{(i)}(\mathcal{W}, \mathcal{B})) \tag{1.36}$$

where L_t is an arbitrary loss function at time step t.

The definition takes into account the output for each temporal step, but,

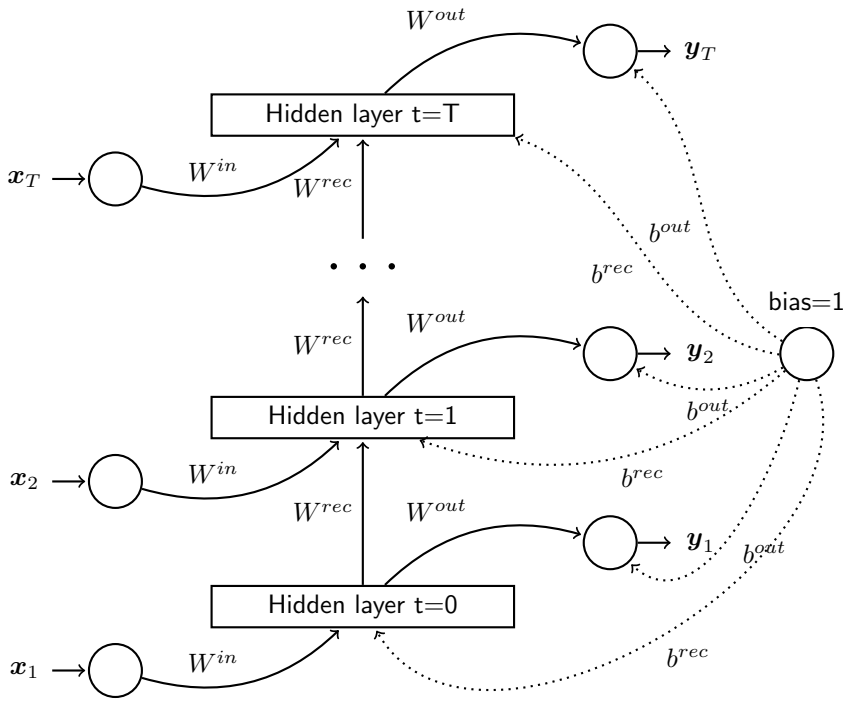

Figure 1.6: Unfolding of a RNN

depending on the task at hand, it could be relevant or not to consider intermediate outputs; that is not a limitation, in fact we could define a loss which is computed only on the last output vector, at time T, and adds 0 for each other time step.

1.3.2 Gradient

Consider a RNN $= \langle \mathcal{W}, \mathcal{B}, \sigma(\cdot), F(\cdot) \rangle$. Let $L_t : \mathbb{R}^o \times \mathbb{R}^o \to \mathbb{R}$ a loss function and $g_t(\cdot) : \mathbb{R}^{\mathcal{N}(\mathcal{W})+\mathcal{N}(\mathcal{B})} \to \mathbb{R}$ be the function defined by

$$g_t(\mathcal{W}, \mathcal{B}) \triangleq L_t(F(\boldsymbol{z}^t(\mathcal{W}, \mathcal{B})))$$

and

$$g(\mathcal{W}, \mathcal{B}) \triangleq \sum_{t=1}^{T} g_t(\mathcal{W}, \mathcal{B})$$

$$\frac{\partial g}{\partial W^{rec}} = \sum_{t=1}^{T} \nabla L_t^T \cdot J(F) \cdot \frac{\partial \boldsymbol{z}^t}{\partial \boldsymbol{a}^t} \cdot \frac{\partial^+ \boldsymbol{a}^t}{\partial W^{rec}} \tag{1.37}$$

$$= \sum_{t=1}^{T} \frac{\partial g_t}{\partial \boldsymbol{a}^t} \cdot \frac{\partial^+ \boldsymbol{a}^t}{\partial W^{rec}} \tag{1.38}$$

As we noticed for FNNs it's easy to compute $\frac{\partial g_t}{\partial \boldsymbol{a}^t}$ once we define $F(\cdot)$ and $L(\cdot)$, note that the weights are not involved in such computation. Let's see how to compute $\frac{\partial \boldsymbol{a}^t}{\partial W^{rec}}$.

Let's consider a single output unit u, and a weight w_{lj}, we have

$$\frac{\partial a_u^t}{\partial w_{lj}} = \sum_{k=1}^{t} \frac{\partial a_u^t}{\partial a_l^k} \cdot \frac{\partial a_l^k}{\partial w_{lj}} \tag{1.39}$$

$$= \sum_{k=1}^{t} \delta_{lu}^{tk} \cdot \phi_j^{t-1} \tag{1.40}$$

where

$$\delta_{lu}^{tk} \triangleq \frac{\partial a_u^t}{\partial a_l^k}. \tag{1.41}$$

Let's observe a first difference from FFNN case: since the weights are shared in each unfolded layer, in equation 1.39 we have to sum over time.

Let $P(l)$ be the set of parents of neuron l, defined as the set of parents in the unfolded network.

$$\delta_{lu}^{tk} = \sum_{h \in P(l)} \delta_{hu}^{tk} \cdot \sigma'(a_h^{t-1}) \cdot w_{hl} \tag{1.42}$$

In Figure 1.7 we can see the arcs which are involved in the derivatives in the unfolded network.

In matrix notation we have:

$$\frac{\partial \boldsymbol{a}^t}{\partial W^{rec}} = \sum_{k=1}^{t} \frac{\partial \boldsymbol{a}^t}{\partial \boldsymbol{a}^k} \cdot \frac{\partial^+ \boldsymbol{a}^k}{\partial W^{rec}} \tag{1.43}$$

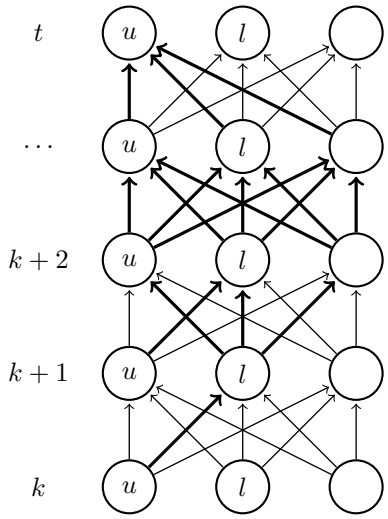

Figure 1.7: Nodes involved in $\frac{\partial a_u^t}{\partial a_l^k}$.

$$\frac{\partial^+ a^k}{\partial W_j^{rec}} = \begin{bmatrix} \phi_j^k & 0 & \cdots & \cdots & 0 \\ 0 & \phi_j^k & \cdots & \cdots & 0 \\ \vdots & \vdots & \ddots & \vdots & \vdots \\ 0 & \cdots & \cdots & \cdots & \phi_j^k \end{bmatrix} \tag{1.44}$$

$$\frac{\partial \boldsymbol{a}^t}{\partial \boldsymbol{a}^k} \triangleq \Delta^{tk} \tag{1.45}$$

$$\Delta^{tk} = \Delta^{t(k+1)} \cdot diag(\sigma'(\boldsymbol{a}^k)) \cdot W^{rec} \tag{1.46}$$

$$= \prod_{i=t-1}^{k} diag(\sigma'(\boldsymbol{a}^i)) \cdot W^{rec}. \tag{1.47}$$

The derivatives with respect to W^{in} and $\boldsymbol{b}^{rec}$ have the same structure. The derivatives with respect to W^{out}, b^{out} are straightforward:

$$\frac{\partial \boldsymbol{g}}{\partial W^{out}} = \sum_{t=1}^{T} \frac{\partial g_t}{\partial \boldsymbol{y}^t} \cdot J(F) \cdot \frac{\partial \boldsymbol{z}^t}{\partial W^{out}} \tag{1.48}$$

$$\frac{\partial \boldsymbol{g}}{\partial \boldsymbol{b}^{out}} = \sum_{t=1}^{T} \frac{\partial g_t}{\partial \boldsymbol{y}^t} \cdot J(F) \cdot \frac{\partial \boldsymbol{z}^t}{\partial \boldsymbol{b}^{out}}. \tag{1.49}$$

Back-propagation through time (BPTT) *Back-propagation through time* is an extension of the *back-propagation* algorithm we described for FNNs. We can think of BPTT simply as a standard BP in the unfolded network. The same considerations done for BP also apply for BPTT, the difference is, of course, in how derivatives are computed. Time complexity is easily derived noticing that in the unfolded network there are $n \cdot T$ units, where n is the number of units of the RNN. This yields time complexity $\mathcal{O}(\mathcal{N}(\mathcal{W}) \cdot T)$. Please see [33] for more details.

1.4 Activation functions and gradient

Activation functions play a central role in artificial neural networks as they are responsible for the non linearity of the model. In the history of neural networks several activation functions have been proposed and used. In the following some of them are taken into consideration, underling the difference between them, with a special focus on their derivative expression.

A special class of activation function, is that of *squashing* functions.

Definition 5. A function $f(\cdot) : \mathbb{R} \to [a, b]$ with $a, b \in \mathbb{R}$ is said to be a *squashing* function if it is not decreasing and

$$\lim_{x \to +\infty} f(x) = b \tag{1.50}$$

$$\lim_{x \to -\infty} f(x) = a. \tag{1.51}$$

Step function, ramp function and all sigmoidal functions are all examples of squashing functions.

Remark 3. An important property of a *squashing* function $\sigma(\cdot)$ is that

$$\lim_{\alpha \to +\infty} \sigma(\alpha \cdot (x - \tau)) = \begin{cases} b \cdot \sigma_\tau(x) & \text{if } x > \tau, \\ a + \sigma_\tau(x) & \text{otherwise,} \end{cases} \tag{1.52}$$

being σ_τ the usual step function. This property is extensively used in several proofs of the universal approximator property of neural networks. Roughly speaking we can say that *squashing* functions act as step functions at the limit.

This property has a practical use since inputs of activation functions are the weighted sum of neurons output, so activation function inputs can be arbitrarily big or small.

Sigmoid

$$sigmoid(x) = \frac{1}{1+e^{-x}}, \tag{1.53}$$

$$\frac{d}{dx} sigmoid(x) = sigmoid(x) \cdot (1 - sigmoid(x)). \tag{1.54}$$

As we can see from Figure 1.8 the sigmoid derivative has only one maximum in 0 where it assume value 0.25. Receding from 0, in both direction leads to regions where the the derivative take zero value, such regions are called *saturation* regions. If we happen to be in such regions, for a given neuron, we cannot learn anything since that neuron doesn't contribute to the gradient.

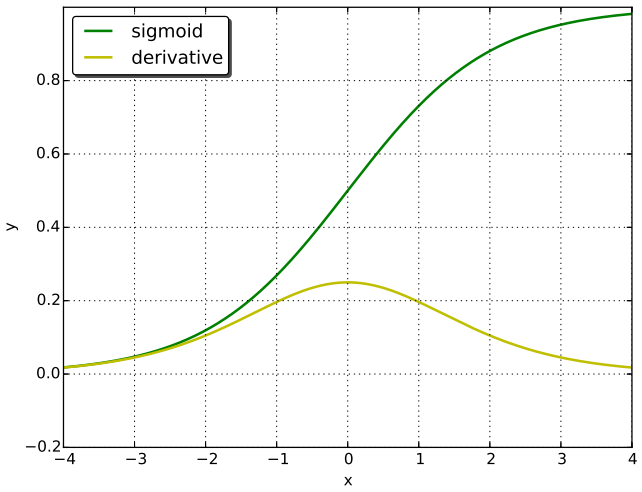

Figure 1.8: sigmoid and its derivative

Tanh

$$tanh(x) = \frac{e^{x} - e^{-x}}{e^{x} + e^{-x}}, \tag{1.55}$$

$$\frac{d}{dx} tanh(x) = 1 - tanh^{2}(x). \tag{1.56}$$

As we can see from Figure 1.9 *tanh* (and it's derivative) have a behavior similar to the sigmoid one; again we have two saturation region towards infinity: that is typical of all squashing functions.

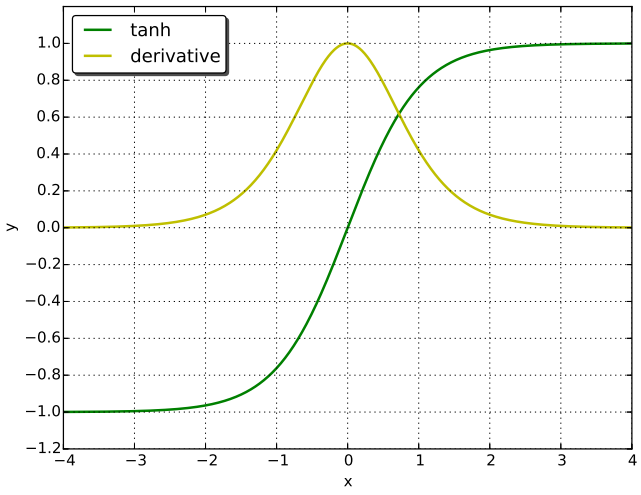

Figure 1.9: tanh and its derivative

ReLU

$$ReLU(x) = \begin{cases} x & \text{if } x > 0. \\ 0 & \text{otherwise.} \end{cases} \tag{1.57}$$

$$\frac{d}{dx} ReLU(x) = \begin{cases} 1 & \text{if } x > 0. \\ 0 & \text{otherwise.} \end{cases} \tag{1.58}$$

ReLU is a bit different from the activation function seen so far: the main difference is that is not a squashing function. As we can see from Figure 1.10, ReLU's derivative is the step function; it has only one *saturation* region $(-\infty, 0]$ and a region in which is always takes value 1, $(0, +\infty]$. This implies that we cannot learn to *turn on* a switched off neuron ($x < 0$), but we have no *saturation* region toward infinity.

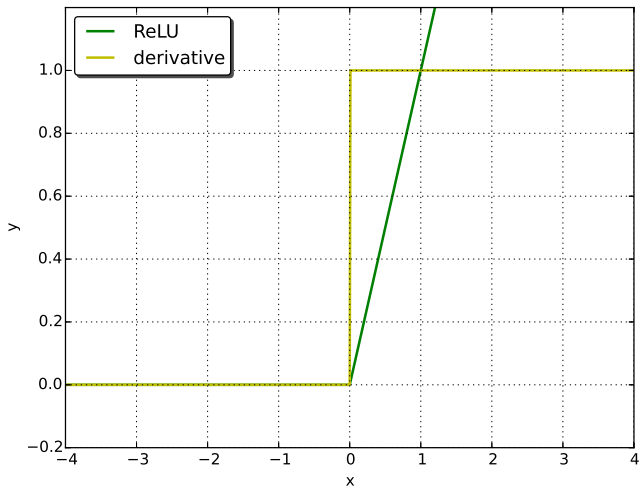

Figure 1.10: ReLU and its derivative

1.5 Stochastic gradient descent: a common framework

In this section we will describe a framework based on gradient descent optimization method which can be used to train neural network of any kind. Such framework constitutes the core of many learning methods used in today's applications. Suppose we have a training set of pairs $D = \{\langle \boldsymbol{x}^{(i)}, \boldsymbol{y}^{(i)} \rangle\}$ and a loss function $L(\theta)$ where θ represents all the parameters of the network.

A standard gradient descend would update θ at each iteration using the gradient computed on the whole training set, as shown below.

$$\theta = \theta - \alpha \nabla_\theta L(\theta). \tag{1.59}$$

This can be very slow or even impractical if the training set is too huge to fit in memory. Stochastic gradient descent (SGD) overcome this problem taking into account only a part of the training set for each iteration, i.e. the gradient is computed only on a subset I of training examples.

$$\theta = \theta - \alpha \nabla_\theta L(\theta; I). \tag{1.60}$$

The subset of training examples used for the update is called *mini-batch*. The number of examples for each mini-batch is an important hyper-parameter because it affects both the speed of convergence in terms of number of iterations and time needed for each iteration. At each iteration new examples are chosen among the training set, so it could, and it always does if we have a finite data-set, happen, that all training set examples get used. This is not a problem, since we can use the same examples over and over again. Each time we go over the entire training set we say we completed and *epoch*. It is not unusual to iterate the learning algorithm for several epochs before converging.

The method is summarized in algorithm 1.1.

Algorithm 1.1: Stochastic gradient descent

Data:
$D = \{\langle \boldsymbol{x}^{(i)}, \boldsymbol{y}^{(i)} \rangle\}$: training set
θ_0: candidate solution
m: size of each mini-batch

Result:
θ: solution

```
θ ← θ_0
while stop criterion do
    I ← select m training example ∈ D
    α ← compute learning rate
    θ ← θ − α∇_θ L(θ; ⟨x^(i), y^(i)⟩, i ∈ I)
end
```

In the following paragraphs we will analyze in more detail each step of the method, surveying the different alternatives that can be used.

The stop criterion Usually a gradient based method adopts a stop criterion which allows the procedure to stop when close enough to a (local) minimum, i.e $\nabla_\theta L(\theta) = 0$. This could easily lead to over-fitting, so is common practice to use a cross-validation technique. The most simple approach to cross-validation is to split the training set in two parts, one actually used as a pool of training examples, which will be called *training set*, and the other, called *validation-set*, used to decide when to stop.

Being $D = \{\langle \boldsymbol{x}^{(i)}, \boldsymbol{y}^{(i)} \rangle, i \in (1, M)\}$ a generic subset of the data-set, we can define the *error* on such set in a straightforward manner as

$$E_D = \frac{1}{M}\sum_{i=1}^{M} L(\boldsymbol{x}^{(i)}, \boldsymbol{y}^{(i)}) \tag{1.61}$$

Since training examples are sampled from the training-set, the error on the training-set will always[2] be decreasing across iterations. The idea behind cross-validation is to compute, and *monitor* the error on the validation set, since it's not guaranteed at all that the error would be decreasing. On the contrary, tough error will generally decrease during the first part of training, it will reach a point when it will start to increase. This is the point when we need to stop training since we are starting to over-fitting. Of course this is an ideal situation, in real applications the validation error could have a more irregular trend, but the idea holds.

Learning rate The parameter α in Equation (1.60) is usually referred to as *learning rate*. Of course the strategy employed to compute such learning rate is an important ingredient in the learning method. The most easy, and often preferred, strategy is that of **constant learning rate**. The learning rate α becomes another hyper-parameter of the network that can be tuned, but it remains constant, usually a very small value, across all iterations.

Another popular strategy is that of **momentum** which, in the optimization field is know as the *Heavy Ball* method [26]. The main idea behind momentum is to accelerate progress along dimensions in which gradient consistently point to and to slow down progress along dimensions where the sign of the gradient continues to change. This is done by keeping track of past parameter updates with an exponential decay as shown in Equation (1.62).

$$v = \gamma v + \alpha \nabla_\theta L(\theta; \langle \boldsymbol{x}^{(i)}, \boldsymbol{y}^{(i)} \rangle, i \in I) \tag{1.62}$$

$$\theta = \theta + v \tag{1.63}$$

Another way of choosing the learning rate is to fix an initial value and **annealing** it, at each iteration (or epoch), according to a policy, for instance

[2]This is not actually true; it would in a standard gradient descent, but since we are using stochastic gradient the error could be non monotonic decreasing. However the matter here is that error mainly follow a decreasing path

exponential or *linear* decay; the idea behind it being that, initially, when far from a minimum having a larger learning rate causes greater speed and after some iterations when approaching a minimum a smaller learning rate allows a finer refinement.

Adaptive methods, instead, choose the learning rate monitoring the objective function, hence learning rate can be reduced or increased depending on the need, proving to be a little more versatile than annealing methods. Of course different strategies for detecting when to reduce or increase the learning rate have been devised.

Finally **line search** which is generally used when working with (non stochastic) gradient descend or when dealing with large batches. For stochastic gradient with small batches other strategies are usually preferred.

How to choose batches Empirical evidence has been provided that choosing a "meaningful" order in which examples are presented to the network can both speed the convergence and yield better solutions. Generally speaking, the network can learn faster if trained first with easier examples and then with examples with gradually increasing difficulty, as humans or animals would do. The idea was introduced by Bengio et al. [3] in 2009, as *curriculum* learning. Experiments on different curriculum strategies can be found in [34].

1.6 The vanishing and exploding gradient problem

As noted in Bengio et al. [4] and Hochreiter [11] the training of recurrent neural networks is afflicted by the *exploding* and *vanishing* gradient problem, namely the norm of the gradient in recurrent neural network tends either to vanish or explode. As we have seen the gradient is composed of terms of the form:

$$\frac{\partial \boldsymbol{a}^t}{\partial \boldsymbol{a}^k} = \prod_{i=t-1}^{k} diag(\sigma'(\boldsymbol{a}^i)) \cdot W^{rec}. \tag{1.64}$$

The terms $\frac{\partial \boldsymbol{a}^t}{\partial \boldsymbol{a}^k}$ capture the "dependecy" of neurons at time step t from neurons at time k. Such term are usually distinguished between *long term* contributions

when $k \ll t$ and *short term* contributions otherwise. We can notice that each temporal contribution is the product of $l = t - k - 1$ matrices, so in *long term* components, where l can be very large, we can intuitively understand that such product can go exponentially fast towards 0 or infinity depending on the spectral radius of the matrices involved.

The *vanishing* gradient problem is directly linked to the notion of memory; when the term $\frac{\partial \boldsymbol{a}^t}{\partial \boldsymbol{a}^k}$ approaches zero value changes in the output of the neurons at time k have little impact on the output at time t. This, in turn, leads to the fact that the output of the net does not depend on inputs of distant temporal steps, i.e. the output sequence is determined only by recent temporal input: we say that the network doesn't have memory. Evidently this can have catastrophic effects on the classification error. Imagine we would like to classify an input sequence as positive whether or not it contains a given character. It would seem a rather easy task, however, if when training the network, we incur in the *vanishing* gradient, we may train a network which performs the classification using only the most recent temporal inputs. What if the character was at the beginning of the sequence? Of course the prediction would be wrong.

Exploding gradient seems to be a rather different kind of a problem, it does not affect the ability of the network to use information from distant temporal steps, on the contrary we have very strong information about where to go using the gradient direction. *Exploding* gradient can be a problem if we intend to use a constant step (think for example of SGD), or even, for example, some decaying policy : if we are to compute a step in the gradient direction with a fixed step and the gradient has too big norm we may make a too big step which may completely ruin the learning process.

Let's now return to the nature of the problem and try to explaining the mechanics of it.

Hochreiter Analysis: A weak upper bound In this paragraph we report some useful considerations made by Hochreiter, please see [11] for more details. Let's put:

$$\|A\|_{max} \triangleq \max_{i,j} |a_{ij}|$$

$$\sigma'_{max} \triangleq \max_{i=k,\dots,t-1} \{\left\| diag(\sigma'(a^i)) \right\|_{max}\}.$$

Since

$$\|A \cdot B\|_{max} <= r \cdot \|A\| \cdot \|B\|_{max} \qquad \forall A, B \in \mathbb{R}_{r\times r}, \tag{1.65}$$

it holds:

$$\left\| \frac{\partial \boldsymbol{a}^t}{\partial \boldsymbol{a}^k} \right\|_{max} = \left\| \prod_{i=t-1}^{k} diag(\sigma'(\boldsymbol{a}^i)) \cdot W^{rec} \right\|_{max} \tag{1.66}$$

$$\leq \prod_{i=t-1}^{k} r \cdot \left\| diag(\sigma'(\boldsymbol{a}^i)) \right\|_{max} \cdot \|W^{rec}\|_{max} \tag{1.67}$$

$$\leq \left(r \cdot \sigma'_{max} \cdot \|W^{rec}\|_{max} \right)^{t-k-1} \tag{1.68}$$

$$= \tau^{t-k-1} \tag{1.69}$$

where

$$\tau \triangleq r \cdot \sigma'_{max} \cdot \|W^{rec}\|_{max} .$$

So we have exponential decay if $\tau < 1$. We can match this condition if $\|W^{rec}\|_{max} \leq \frac{1}{r \cdot \sigma'_{max}}$. As pointed out by Hochreiter in his work, in the case of sigmoid activation function, we have $\|W^{rec}\|_{max} < \frac{1}{0.25 \cdot r}$.

Note that we would actually reach this upper bound for some i, j only if all the path cost have the same sign and the activation function takes always maximal value.

An upper bound with singular values Lets decompose W^{rec} using the singular value decomposition. We can write

$$W^{rec} = S \cdot D \cdot V^T \tag{1.70}$$

where S, V^T are squared orthogonal matrices and $D \triangleq diag(\mu_1, \mu_2, ..., \mu_r)$ is the diagonal matrix containing the singular values of W^{rec}. Rewriting Equation (1.64) using this decomposition leads to

$$\frac{\partial \boldsymbol{a}^t}{\partial \boldsymbol{a}^k} = \prod_{i=t-1}^{k} diag(\sigma'(\boldsymbol{a}^i)) \cdot S \cdot D \cdot V^T. \tag{1.71}$$

Since U and V are orthogonal matrix, hence

$$\|U\|_2 = \left\|V^T\right\|_2 = 1,$$

and

$$\|diag(\lambda_1, \lambda_2, ..., \lambda_r)\|_2 \leq \lambda_{max},$$

we get

$$\left\|\frac{\partial \boldsymbol{a}^t}{\partial \boldsymbol{a}^k}\right\|_2 = \left\|(\prod_{i=t-1}^{k} diag(\sigma'(\boldsymbol{a}^i)) \cdot S \cdot D \cdot V^T)\right\|_2 \tag{1.72}$$

$$\leq (\sigma'_{max} \cdot \mu_{max})^{t-k-1}. \tag{1.73}$$

The previous equation provide a sufficient condition, $\sigma'_{max} \cdot \mu_{max} < 1$, as in Hochreiter's analysis, for exponential decay of long term components. In this case however the bound depends on the singular value of the recurrent weights rather than on the maximal weight of the matrix itself.

A similar result is obtained in [25], where W^{rec} is supposed to be diagonalizable; the founding is that a sufficient condition for the gradient to vanish is $\lambda_{max} < \frac{1}{\sigma'_{max}}$ where λ_{max} is the largest eigen value. Please note that in case W^{rec} is diagonalizable $\lambda_{max} = \mu_{max}$, hence our results are more general.

Explaining the problem using the network's graph Let's now dig a bit deeper and rewrite Equation (1.64) with respect to a couple of neurons i and j.

$$\frac{\partial \boldsymbol{a}_i^t}{\partial \boldsymbol{a}_j^k} = \sum_{q \in P(j)} \sum_{l \in P(q)} \dots \sum_{h:i \in P(h)} w_{qj} \dots w_{jh} \cdot \sigma'(a_j^k)\sigma'(a_q^{k+1}) \dots \sigma'(a_i^{t-1}) \tag{1.74}$$

Observing the previous equation we can argue that each derivatives it's the sum of p^{t-k-1} terms; each term represents the path cost from neuron i to neuron j in the unfolded network, obviously there are p^{t-k-1} such paths. If we bind the cost $\sigma'(a_l^t)$ to neuron l in the t^{th} layer in the unfolded network we can read the path cost simply surfing the unfolded network multiply the weight of each arc we walk through and the cost of each neuron we cross, as we can see from Figure 1.11.

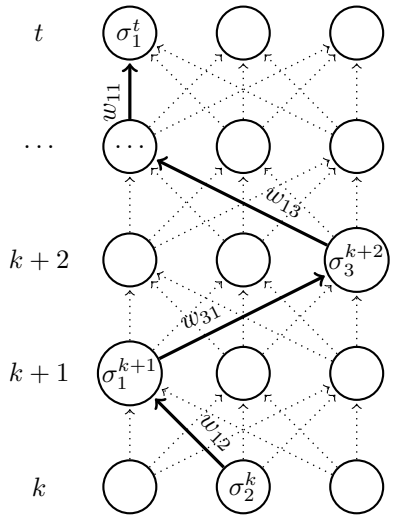

Figure 1.11: The cost for a path from neuron 2 at time k to neuron 1 at time t is $w_{12}w_{31}w_{13}\dots w_{11}\cdot\sigma_2^k\sigma_1^{k+1}\sigma_3^{k+2}\dots\sigma_1^{t-1}$.

We can further characterize each path cost noticing that we can separate two components, one that depends only on the weights $w_{qj}\dots w_{jh}$ and the other that depends both on the weights and the inputs $\sigma'(a_j^k)\sigma'(a_q^{k+1})\dots\sigma'(a_i^{t-1})$.

The ReLU case ReLU case is a bit special, because of its derivative. ReLU's derivative is the step function, it can assume only two values: 1 when the neuron is active, 0 otherwise. Returning to the path graph we introduced earlier we can say that a path is *enabled* if each neuron in that path is active. In fact if we encounter a path which cross a non active neuron it's path cost will be 0; on the contrary for an *enabled* path the cost will be simply the product of weight of the arcs we went through, as we can see in Figure 1.12

So $|(\frac{\partial \boldsymbol{a}^t}{\partial \boldsymbol{a}^k})_{ij}|$ ranges from 0, when no path is enabled to, $|((W^{rec})^{t-k-1})_{ij}|$ when all paths are enabled and all path cost have the same sign, which is consistent with what we found in Hochreiter analysis. We can argue then that ReLU has an advantage over sigmoidal activation functions, for instance, because gradient depends only on the W^{rec} matrix: ReLU function *only* enables or disables the paths but doesn't change their costs as sigmoids do

Poor solutions Pretend we have found, with some learning technique, an assignment for all the weights which causes the gradient to have close to zero

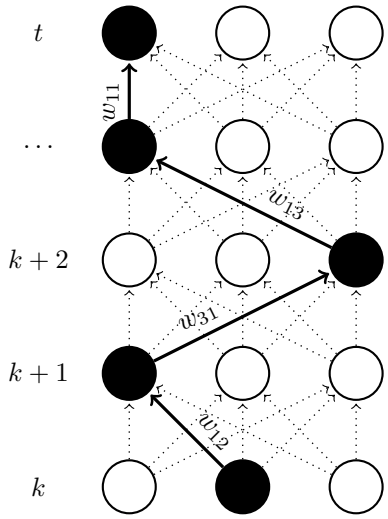

Figure 1.12: The cost for an enabled path from neuron 2 at time k to neuron 1 at time t is $w_{12}w_{31}w_{13}\dots w_{11}$.

norm. We could be happy with it and claim to have "solved" the problem. However, by chance, we discover that $\frac{\partial \boldsymbol{a}^T}{\partial \boldsymbol{a}^k}$ has zero norm for all time steps $k < \tau$. So, the output of the network doesn't depend on the inputs of the sequence for those time steps. In other words we have found a possibly optimal solution for the truncated sequence $x_{[\tau:T]}$. The solution we have found is an optimal candidate to be a bad local minimum.

As a final observation on this topic it is worth noticing how a bad initialization of W^{rec} can lead to poor solutions or extremely large convergence time just because such initialization imply $\frac{\partial \boldsymbol{a}^t}{\partial \boldsymbol{a}^k}$ approaching zero norm for $t \gg k$. Moreover, even if we somehow provide an initialization matrix which is unaffected by this curse, it is certainly possible that we reach such a bad matrix during the learning phase. Several techniques have been proposed to overcome this problem, they will be the topic of later chapters.

1.7 On expressiveness

In this section we will investigate the expressive power of neural networks, presenting some results that motivate the use of neural networks as learning models and underline the differences between FNNs and RNNs.

One of the first import results regarding the expressive power of neural net-

works its due to Hornik et al. [12] which states *"Multilayered feed foward networks with at least one hidden layer, using an arbitrary squashing function, can approximate virtually any function of interest to any desired degree of accuracy provided sufficiently many hidden units are available"*.

To give a more formal result we need first to define what *approximate to any degree of accuracy means*. This concept is captured in the following definition

Definition 6. A subset S of $\mathbb{C}^n$ (continuous functions in $\mathbb{R}^n$) is said to be *uniformly dense on compacta in* $\mathbb{C}^n$ if $\forall$ compact set $K \subset \mathbb{R}^n$ holds: $\forall \epsilon > 0$, $\forall g(\cdot) \in \mathbb{C}^n \ \exists f(\cdot) \in S$ such that $\sup_{x \in K} \|f(x) - g(x)\| < \epsilon$

Hornik result is contained in theorem 1.

Theorem 1. For every squashing function σ, $\forall n \in \mathbb{N}$, feed forward neural networks with one hidden layer are a class of functions which is *uniformly dense on compacta in* $\mathbb{C}^n$.

Theorem 1 extends also to Borel measurable functions, please see [12] for more details.

A survey of other approaches, some of which constructive, in the sense that they actually show how to build the networks, which achieve similar results can be found in [28]. We don't know of any results concerning ReLU activation function.

This results implies that FNN are *universal approximators*, this is a strong argument for using such models in machine learning. It is important to notice, however, that the theorem holds if we have *sufficiently many* units. In practice the number of units will be bounded by the machine capabilities and by computational time, of course greater the number of units greater will be the learning time.

Let us now turn our attention to RNNs and see how the architectural changes, namely the addition of backward links, affect the expressive power of the model. It suffice to say that RNNs are as powerful as Turing machine. Siegelman and Sontag [30] proved the existence of a finite neural network, with sigmoid activation function, which simulates a universal Turing machine. Hyötyniemi [13] proved, equivalently, that turing machine are recurrent neural network showing

how to build a network, using instead ReLU activation function, that performs step by step all the instruction of a computer program. Hyötyniemi work is particularly interesting because it shows how to construct a network that simulate an algorithm written a simple language equivalent to a turing machine. For each instruction type (increment, decrement, conditional branching, ...) a particular setting of weights and neuron is devised allowing the net to simulate step by step the behavior of the program. In the program equivalent network there are a unit for each program variable and one or two, depending on the instruction type, units for each program instruction. This is very interesting from an expressiveness point of view since it bounds the number of units we ought to use with the length of the algorithm we are trying to reproduce.

For better understanding the implications of this fact, imagine how many complex function you can express with short algorithms, for example (approximation of) fractals . It is worth underling the difference with feed forward neural networks where a large number of units seems to be required. This seems to suggest that FFNNs and RNNs differ mainly in a manner of representation, where FNNs use space to define a somehow explicit mapping from input to output, RNNs use time to implicitly define an algorithm responsible for such mapping.

This seems extremely good news, since we could simulate turing machines, hence all algorithms we can think of, using a recurrent neural network with a relatively small number of units; recall that for FFNN we had to suppose infinitely many units to obtain the universal approximator property. Of course there is a pitfall: we can simulate any turing machine but we have to allow sufficiently many time steps and choose a termination criterion. This is of course impractical, and we don't use RNNs in this way. Usually the number of time steps is chosen to be equal to the input sequence length. This of course restrict the class of algorithm we can learn with RNNs. In particular the class of algorithms suited to be learned by such models is that of algorithms consisting in at most one loop, i.e $\mathcal{O}(n)$ time, and constant memory. For example we can imagine to learn algorithms which, scanning the input sequences, detect particular patterns, *store* them, and step by step, produce an output based on the patterns detected so far.

Chapter 2

Literature review

Hochreiter [11] in 1991, Bengio et al. [4] in 1994, and others, observed that gradient in deep neural networks tends to either vanish or explode. From then onward several methods have been proposed to overcome what is now know as the *exploding/vanishing gradient* problem. We can roughly partition such methods in two broad categories. The approaches of the first kind, the ones we call *architectural driven*, usually use a simple stochastic gradient descend (SGD) as learning algorithm, and act on the network topology, modifying the way the neural units operates, the connections between them or the relationship between layers; the idea of such methods is to build networks architectures in which gradient are less likely to vanish, or in other words whose units are able to store information for several time steps.

The second approach, which we call *learning driven*, instead, focus on the learning algorithm, leaving the network architecture untouched. Methods belonging to these categories, either employ learning algorithms different from SGD, or they propose modification to the SGD framework.

In the rest of the chapter we will review the most relevant approaches for both the categories.

2.1 Architectural driven methods

2.1.1 Long short-term memory

Long short-term memory (LSTM) were proposed (1997) by Hochreiter and Schmidhuber [11] as a novel network structure to address the vanishing gradient problem, which was first studied by Hochreiter (1991) in his diploma thesis, a milestone of deep learning.

The idea behind this structure is to enforce a constant error flow, that is to say, to have constant gradient norm, thus preventing the gradient to vanish. This is done by introducing special types of neurons called *memory cells* and *gate units*. As we can see by looking at Figure 2.1, a memory cell is essentially a neuron with a self connection with unitary weight, whose input and output are managed by two multiplicative neurons: the gate units.

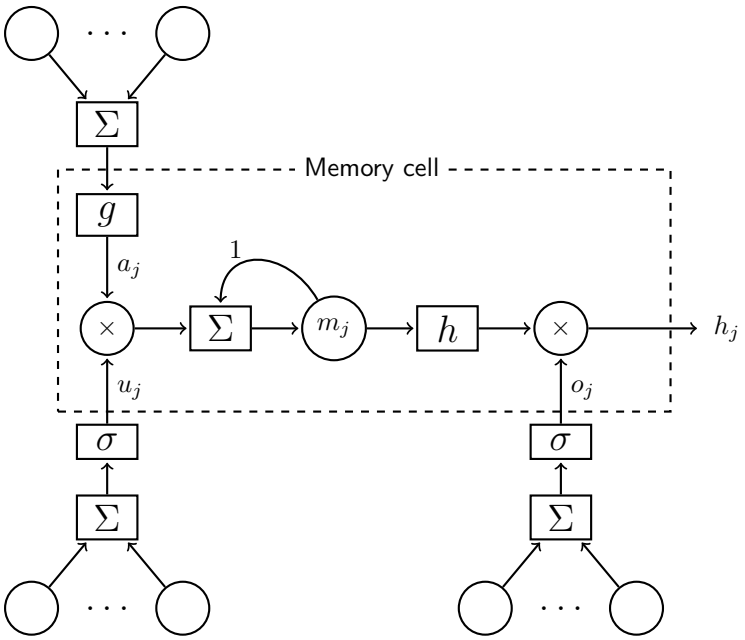

Figure 2.1: Memory cell and gate units of LSTM network.

The memory cell and the gate units behave accordingly to the following:

$$u_j^t = \sigma[W_u \cdot \boldsymbol{x_t} + U_u \cdot \boldsymbol{h}_{t-1}]_j \tag{2.1}$$

$$o_j^t = \sigma[W_o \cdot \boldsymbol{x_t} + U_o \cdot \boldsymbol{h}_{t-1}]_j \tag{2.2}$$

$$a_j^t \triangleq g[W \cdot \boldsymbol{x_t} + U \cdot h_i^t]_j \tag{2.3}$$

$$m_j^t \triangleq a_j \cdot u_j^t + (1 \cdot m_j^{t-1}) \tag{2.4}$$

$$h_j \triangleq h(m_j^t) \cdot o_j^t. \tag{2.5}$$

As we can see from Equation (2.4), the value of the memory cell $m(t)$ remains constant as long as the input gate u does not "open" causing a "write" operation. Similarly the output o of the memory cell, which is connected with the other neurons of the network, is controlled by an output gate: the memory will have a non zero output only if the output gate opens, which we could call a "read" operation. As for constant error flow it is ensured because the memory cell has only a self-loop with unitary weight.

Memory cells, guarded by gate units can be employed in networks with various topology alongside traditionally input, output and hidden units. Another way to look at this kind of architecture is to think of memory cells as units able to store one bit of information, even for long periods of time, hence able to learn distant time correlations between inputs.

As we have seen these network units are specifically designed to store information, through the use of gates; these gates however are no different from other units, apart from the fact they are multiplicative units, hence without further precautions, the networks would incur in the same vanishing problem it aimed to resolve. In fact LSTM comes with a proper, specifically designed, learning algorithm: essentially errors, i.e. gradients of the loss function, arriving at memory cells inputs are not propagated back in time, only the error within the memory cell gets propagated; in other words gradients are truncated taking into account only the self-connection of the memory cells and not its other input connections, hence providing constant error flow.

LSTM units have proven to be very successful reaching state-of-art results in various tasks and even at the present time (2015), they continue to be largely

employed. In recent implementations however, alongside small modifications, as the introduction of other gates, the LSTM architecture is often used without the original learning algorithm which is often replaced by a standard stochastic gradient descend as done in [10].

2.1.2 Gated recurrent units

Gated recurrent units (GRU) were introduced by Cho et al. [6] in 2014 as units similar to LTSM, with the same purpose, but claimed to simpler to compute and implement. A GRU unit j make use of two gate units, z, the *update* gate, and r, the *reset* gate, which are standard neurons.

$$z_j^t = [\sigma(W_z \boldsymbol{x_t} + U_z \boldsymbol{h}_{t-1})]_j \tag{2.6}$$

$$r_j^t = [\sigma(W_r \boldsymbol{x_t} + U_r \boldsymbol{h}_{t-1})]_j. \tag{2.7}$$

$$\tag{2.8}$$

As in LSTM units, the gates manage the access to memory cell, but in GRU they are used a little bit differently. The update gate is used to decide how to update the memory cell: the activation value of the cell h_j^t is a linear interpolation between the previous activation h_j^{t-1} and the candidate activation $\tilde{h}_j^t$.

$$h_j^t \triangleq (1 - z_j^t) h_j^{t-1} + z_j^t \tilde{h_j^t} \tag{2.9}$$

$$\tilde{h}_j^t = [\sigma(W \boldsymbol{x_t} + U(\boldsymbol{r}_t \odot \boldsymbol{h}_{t-1})]_j \tag{2.10}$$

where $\odot$ symbolize the element-wise product.

As we can see from Equation (2.10), when the reset gate r_j^t is close to zero, the units acts as if reading the first symbol of the input sequence *forgetting* the previous state.

Architecture comparison LSTM and GRU present very similarities, the most relevant one being the additive mechanism of update which helps the networks to store information during several time step. One difference between the two architectures is, instead, the lacking of an output gate in GRU, which hence expose the content of the memory cell without any supervision. In [7] Cho

et al. compare the two architectures showing how a gated architecture improves the performance of a network composed of traditional units; The comparison results obtained were however mixed, and in the end they could not demonstrate the superiority of one of the two approaches.

In 2015 an interesting work [15] was done on neural network architectures. The aim of the work was to determine if LSTM or GRU were optimal, or whether a better architecture exists. This was accomplished by comparing thousands of randomly generated architectures using the best hyper-parameter setting for each one. The architectures were generated randomly mutating a given architecture, replacing its activation function nodes, choosing from ReLU, tanh, sigmoid etc., and its operation nodes, with multiplication, subtraction or addition. The result of the experiment is that no one of mutated architectures constantly performed better than LTSM and GRU in all the considered tasks. Moreover the best randomly generated architectures were very similar to the GRU architecture. The conclusion drawn in [15] is that architectures better than LSTM and GRU either do not exist or are difficult to find.

2.1.3 Structurally constrained recurrent network

In 2015 Mikolov proposed a novel network architecture to deal with vanishing gradients [21] called *Structurally constrained recurrent network* (SCRN). The idea is to introduce a hidden layer specifically designed to capture long-term dependencies alongside the traditional one as shown in Figure 2.2.

As observed in [21], and explained in section 1.6, gradient can vanish either because of the non linearities being all close to 0 or because of the multiplication of the weight matrix at each time step. The proposed layer, called *context layer*, address these problem by completely removing the non linearity and forcing the recurrent matrix to be close to the identity. Formally the context layer $\boldsymbol{s}$ is given by:

$$\boldsymbol{s}_t = (1 - \alpha)B\boldsymbol{x}_t + \alpha\boldsymbol{s}_{t-1}. \tag{2.11}$$

The rest of the network is like a traditional one, hence, adding the context

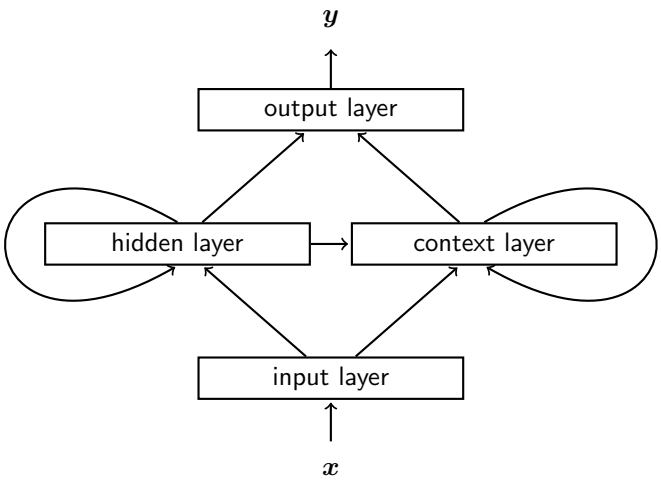

Figure 2.2: SCRN architecture.

layer beside the traditional one results in:

$$\boldsymbol{h}_t = \sigma(P\boldsymbol{s}_t + A\boldsymbol{x}_t + R\boldsymbol{h}_{t-1}) \tag{2.12}$$

$$\boldsymbol{y}_t = f(U\boldsymbol{h}_t + V\boldsymbol{s}_t). \tag{2.13}$$

Notice the similarity with leaky integrator units [14].

If we treat context and traditional layers as one, i.e we do not distinguish between context and traditional units, we can see the model as a traditional model whose recurrent matrix W is constrained (from this the name of the method), to be of the form:

$$W = \begin{bmatrix} R & P \\ 0 & \alpha I \end{bmatrix} \tag{2.14}$$

Matrix W is a traditional recurrent matrix constrained to have a diagonal block to be equal to a weighted identity.

Observing that fixing α to be constant makes the context units to work on the same time scale, Mikolov propose to have a different value for each unit, hence allowing to capture context from different time delay.

$$\boldsymbol{s}_t = (I - Q)B\boldsymbol{x}_t + Q\boldsymbol{s}_{t-1} \tag{2.15}$$

where $Q \triangleq diag(\sigma(\boldsymbol{\beta}))$; the vector $\boldsymbol{\beta}$ is learned.

In [21] SCRNs are shown to be roughly equivalent to the much more complex, LSTMs.

2.1.4 Gated feedback recurrent neural networks

Gated feedback recurrent neural networks were proposed in 2015 by Chung et al. [8] as a novel recurrent network architecture. Unlike LSTM or GRU where the novelty of the proposal was a new kind of unit, designed to better capture long-term dependencies between inputs, the novelty of this approach is the way the units are arranged. For starters multiple recurrent layer are used, like in a *Stacked RNN*, i.e. the network is composed of several layers, each one of which is connected to all the others; in other words the layers are fully connected. Moreover, unlike traditional stacked RNNs, the feedback connection between different layers is gated by a *global reset gate* which is essentially a logistic unit computed on the current inputs and the previous states of hidden layers. This global reset gates is reminiscent of the gates of LSTM and GRU but it controls the connection between layers not between units: the hidden state values of layer i at time $t-1$ are fed to a lower layer j multiplied by $g^{i\to j}$. The gate between layers i and j is computed as:

$$g^{i\to j} \triangleq \sigma(\boldsymbol{w}_g^{i\to j} \cdot \boldsymbol{h_t}^{j-1} + \boldsymbol{u}_g^{i\to j} \cdot \boldsymbol{h}_{t-1}^{*}) \tag{2.16}$$

where $\boldsymbol{w}_g^{i\to j}$ and $\boldsymbol{u}_g^{i\to j}$ are the weights of the links between the gate and the input and the hidden states of all layers at time-step $t-1$ respectively; for $j=1$, $\boldsymbol{h}_t^{j-1} = \boldsymbol{x}_t$ and $\boldsymbol{h_{t-1}^{*}}$ represents all the hidden states at time $t-1$.

The idea behind this architecture is to encourage each recurrent layer to work at different timescales, hence capturing both long-term and short-term dependencies. In addition, the units composing the layers, can be traditional sigmoidal units but also LSTM or GRU, hence benefiting from both the strength of these kind of units and the global gate mechanism. In [8] the architecture is evaluated against traditional and stacked RNNs with both LSTM and GRU units: gated feedback networks are shown to offer better performance and accuracy in several challenging tasks.

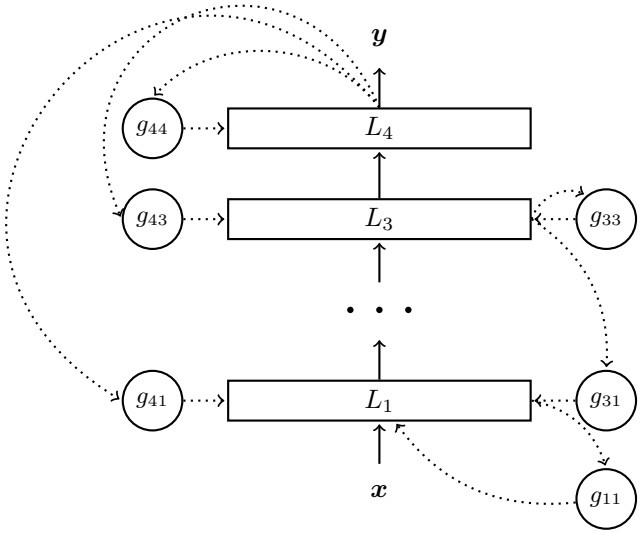

Figure 2.3: Gated feedback architecture. Only connections between layers are shown, dotted when trough gates.

2.2 Learning driven methods

2.2.1 Preserve norm by regularization and gradient clipping

In 2013 Pascanu [25] proposed a regularization term Ω for the loss function $L(\theta)$ which should address the vanishing gradient problem. The objective function hence become:

$$\tilde{L}(\theta) \triangleq L(\theta) + \lambda\Omega(\theta) \tag{2.17}$$

Such a term represents a preference for solutions such that back-propagated gradients preserves norm in time.

$$\Omega = \sum_t \left(\frac{\left\| \frac{\partial L}{\partial \boldsymbol{h}_{t+1}} \cdot \frac{\partial \boldsymbol{h}_{t+1}}{\partial \boldsymbol{h}_t} \right\|}{\left\| \frac{\partial L}{\partial \boldsymbol{h}_{t+1}} \right\|} - 1 \right)^2 \tag{2.18}$$

As we can see from equation 2.18 the regularization term forces $\frac{\partial \boldsymbol{h}_{t+1}}{\partial \boldsymbol{h}_t}$ to

preserve norm in the relevant direction of the error $\frac{\partial L}{\partial \boldsymbol{h}_{t+1}}$.

The intuition behind this technique is that $\frac{\partial \boldsymbol{h}_t}{\partial \boldsymbol{h}_k}$ measure the dependence of outputs at time t on the previous time steps $t-1, ...k$. In [25] is argued that even though some precedent inputs $k < t$ will be irrelevant for the prediction of time time t, the network cannot learn to ignore them unless there is an error signal; hence it's a good idea to force the network to increase $\frac{\partial \boldsymbol{h}_t}{\partial \boldsymbol{h}_k}$, even at the expense of greater error of the loss function $L(\theta)$, and then wait for it to learn to ignore these inputs.

As for the exploding vanishing gradient, in [25] is argued that a simple method called *gradient clipping*, first used by Mikolov [20], can be effective against exploding gradient. The method, shown in algorithm 2.1, simply consists in rescale the gradient norm when it goes over a threshold.

Algorithm 2.1: Gradient clipping

```
g ← ∇_θ L
if ‖g‖ ≥ threshold then
    g ← (threshold / ‖g‖) g
end
```

A drawback of such an approach is the introduction of another hyper-parameter, the threshold, however in [25] is said that a good heuristic is to choose a value from half to ten times the average gradient norm over a sufficiently large number of updates. The algorithm can be described also in terms of adjusting the learning rate monitoring the gradient. Our understanding is that such escamotage is not necessary at all when, for instance, using a line search algorithm for setting the learning rate.

2.2.2 Hessian-free optimization

During 2010-2011 Martens and Sutskever [19] proposed an developed an hessian-free method for recurrent neural network training. The proposal consists in using Hessian-free optimization with some crucial modifications which make the approach suitable for recurrent neural networks.

As in the classical Newton's method the idea is to iteratively compute the updates to parameter θ by minimizing a local quadratic approximation $M_k(\delta)$ of the objective function $f(\theta_k + \delta)$, which in the case of RNNs is the loss function

$L(\theta)$, as shown in equation 2.19.

$$M_k(\delta) = f(\delta_k) + \nabla f(\delta_k)^T \delta + \frac{1}{2}\delta^T B_k \delta \tag{2.19}$$

where B_k is the curvature matrix, which in the standard Newton matrix would the Hessian $\nabla^2 f(x_k)$. The update of the parameter δ is given by:

$$\theta_{k+1} = \alpha_k \delta_k^* \tag{2.20}$$

where δ_k^* is the minimum $M_k(\delta)$ and $\alpha_k \in [0, 1]$ is chosen typically via line-search.

The use of the Hessian is however impractical for several reason: first of all if not positive definite $M(\delta_k)$ will not be bounded below; moreover even if positive definite, computing $\delta_k^* = \delta_k - B_{k-1}^{-1} \nabla f(\delta_{k-1})$, as in standard Newton, can be too much computationally expensive.

Gauss-Newton curvature matrix The proposal of [19] for indefiniteness is to use the generalized Gauss-Newton matrix (GGN) proposed by Schraudolph [29] as an approximation of the Hessian. As for the computational cost of the matrix inversion it is addressed, as in Truncated-Newton methods, by partially minimizing the quadratic function $M_k(\delta)$ using the conjugate gradient algorithm. CG is usually stopped early, before convergence, and it is "hot started": the method is initialized with the (approximate) solution of the previous quadratic approximation.

Let decompose the objective function $f(\theta)$ in $L(F(\theta))$ using the usual loss function $L(\cdot)$ and the output vectorial valued function of the network $F(\theta)$. Is required that $L(\cdot)$ is convex. The GNN can be derived as follows:

$$\nabla f(\theta) = J(F)^T \nabla L \tag{2.21}$$

$$\nabla^2 f(\theta) = J(F)^T \nabla^2 L J(F) + \sum_{i=1}^{m} [\nabla L]_i \cdot [\nabla^2 F_i] \tag{2.22}$$

The GNN is defined as:

$$GNN \triangleq J(F)^T \nabla^2 L J(F). \tag{2.23}$$

GNN is positive definite, provided $L(\cdot)$ is convex, and it easy to see that GNN is the Hessian of $f(\theta)$ if $F(\theta)$ is replaced by it's first order approximation.

Damping As observed in [19], Newton's method is guaranteed to converge to a local minimum only if initialized sufficiently close to it. In fact, the minimum of the quadratic approximation $M_k(\delta)$, can be far beyond the region where $M_k(\delta)$ is a "reliable" approximation of $f(\theta_k + \delta)$. For this reason applying the previously described method to highly non linear objective function, as in the case of RNNs, can lead to very poor results. A solution to overcome this problem can be using a first order method as stochastic gradient descend, to reach a point close enough to a minimum and the switch to Hessian-free optimization for finer convergence. In [19] however is argued that making use of the curvature can be beneficial in constructing the updates from the beginning.

Damping is a strategy to make use of curvature information as in Newton's like methods, in a more conservative way, so that updates lie in a region where $M_k(\delta)$ remains a reasonable approximation of $f(\theta_k + \delta)$. A classic damping strategy is Tikhonov damping; it consists in adding a regularization term to the quadratic approximation:

$$\tilde{M_k}(\delta) \triangleq M_k(\delta) + \frac{\lambda}{2} \|\delta\|^2 \tag{2.24}$$

Of course λ is a very critical parameter, too small values of λ lead to regions where the quadratic doesn't not closely approximate the objective function, conversely, too big values lead to updates similar to that we would have obtained with a first order method. Another important observation is that λ cannot be set once and for all at the beginning of the optimization, but has to be tuned for each iteration. One classic way to compute λ adaptively is to use the Levenberg-Marquardt like heuristic. Let the reduction ration ρ be:

$$\rho \triangleq \frac{f(\theta_k + \delta_{k-1}) - f(\theta_k)}{M_k(\delta_{k-1})} \tag{2.25}$$

The Levenberg-Marquardt heuristic is given by

$$\lambda = \begin{cases} \frac{2}{3}\lambda & \text{if } \rho > \frac{3}{4} \\ \frac{3}{2}\lambda & \text{if } \rho < \frac{1}{4} \end{cases} \tag{2.26}$$

The idea behind this strategy is that when ρ is smaller than 1 the quadratic model overestimate the amount of reduction and so λ should be increased, conversely when ρ is close to 1 the quadratic approximation is accurate and hence we can afford a smaller value of λ.

However in [19] is argued that Tikhonov damping can perform very poorly when applied to RNNs, the reason being that $\|\cdot\|$ is not a reasonable way to measure change in θ; as pointed out in [19] $\|\cdot\|$ works well when the parameters θ operate[1] at roughly the same scale, and that's not certainly the case of RNNs, which, by the way, is also the motivation that urged Martens to try second order methods, and it's linked to the vanishing gradient problem.

To overcame this problem, in [19], a novel damping scheme, called *structural damping*, is proposed. Structural damping consists, as in Tikhonov, in a regularization term which penalizes the directions of change in the parameter space which lead to large changes in the hidden state sequence, which corresponds to highly inaccurate quadratic approximations.

$$\tilde{M}_k(\delta) \triangleq M_k(\delta) + \frac{\lambda}{2}\|\delta\|^2 + \mu D(h(\theta_{k+1}, \theta_k)) \tag{2.27}$$

where $D(\cdot)$ is a distance (or loss) function which measure the variation in the hidden states due to the update of θ as, for example the squared distance.

Since minimization of $\tilde{M}_k(\delta)$ is done by conjugate gradient and such function is not not quadratic, in practice, a Taylor series approximation, along with the use of the Gauss-Newton matrix, is used in place of $D(h(\theta_{k+1}, \theta_k))$.

Minibatching As a last note regarding the proposed method it is important to notice that the method can work in a stochastic fashion, i.e using a small subset (minibatch) of the training examples, like stochastic gradient descend (SGD), for instance. This is a very important feature since datasets are get-

[1] changing a weight in an RNN can have a very little effect in the output function or, conversely, the changes can be substantial, depending on what weight is modified

ting bigger and bigger, hence computing gradients on the whole training set is becoming computationally impractical. However, unlike SGD, where minibatch can be arbitrary small, the proposed method, and all second order methods in general, deteriorate it's performance with too small batches, but that seems to be not much of a problem.

As shown in [19] the proposed Hessian-free optimization method outperforms the previously state-of-art LSTM [11] approach, proving to be able to well managing long-term dependencies. A more detailed theoretical analysis of why such method works is, however, still missing. A possible intuitive explanation can be found in [2, 25].

2.2.3 Reservoir computing

Reservoir Computing is a completely different paradigm to "train" RNNs, and in general models with complex dynamics, proposed independently in 2001 by Herbert Jaeger under the name *Echo State Networks* [17] and by Wolfang Maas under the name *Liquid Machines* [18].

Methods belonging to Reservoir computing family make use of RNNs in the following way: first they *randomly* create a RNN (i.e. they assign the weight matrices), which is called the *reservoir*; then they used the neurons outputs to learn a mapping from input to target sequences. Such methods make a strong conceptual and computational distinction between the *reservoir*, and the *readout* function. It's important to notice that they weights of the RNNs, are not learned in any way;

The interest in such models was raised by the fact that such networks often outperformed state-of-art fully learned RNNs.

The several methods which falls into this category differ in they way they generate the *reservoir* and the type of *readout* mapping they make use of. *Readout* functions can be simple linear functions, maybe preceded by a kernel expansion of the neuron output sequence, a multi-layered FFNN, etc. and they are learned in the usual way. As for the reservoir there are several "recipes" for producing "good" ones: from fully unaware of the training set methods, which randomly generate the RNN, aiming to provide rich dynamics, to meth-

ods which choose a RNN depending on the behavior of such network on the training set. For a more detailed summary of the field please see [16].

Echo state networks *Echo State Networks* (ESN) usually make use of a randomly generated *reservoir* and of linear *readout* function, preceded by a kernel expansion.

The ESN recipe for generating the *reservoir* is to generate a *big*, *sparsely* and *randomly* connected RNN. The aim of this design is to provide to the readout function signals which are different and loosely coupled.

The fundamental element for the ESN architecture to work is that it has to have the *echo state property*: the effect of a previous (hidden) state and input on the future state should vanish gradually as time passes. This is usually accomplished by controlling the spectral radius of the recurrent weight matrix $\rho(W)$. The rule of thumb, given by ESNs inventor Jaeger, is to use $\rho(W)$ close to 1 when dealing with tasks requiring long memory and $\rho(W) < 1$ when dealing with tasks where memory is less important. This reminds a lot of the Hochreiter's conditions for vanishing/exploding gradient (section 1.6).

Another common feature of ESN is the use of a novel neuron model called *leaking integrator neuron*:

$$\boldsymbol{h_t} = (1 - \alpha)\sigma(W^{rec}\boldsymbol{h}_t + W^{in}\boldsymbol{x}_t + b^{rec}) + \alpha\boldsymbol{h}_{t-1} \tag{2.28}$$

The parameter α controls the "speed" of the reservoir dynamics: a small value of α makes the reservoir react slowly to the input, whether a larger value would make the neurons change at faster rate.

2.2.4 Nesterov's accelerated gradient and proper initialization

In 2013 [32] showed how two key elements, namely a proper initialization of the weight matrices and a momentum method for the update rule, could help stochastic gradient descent algorithm to reach performances close the one of state-of-art hessian-free optimization of Martens [19].

Classical momentum [26] consist in the following update rule:

$$v_{t+1} = \gamma v_t + \alpha \nabla_\theta f(\theta_t) \tag{2.29}$$

$$\theta_{t+1} = \theta_t + v_{t+1} \tag{2.30}$$

In [32] is shown how *Nesterov's accelerated gradient* NAG [23] can be see as a modification of the former:

$$v_{t+1} = \gamma v_t + \alpha \nabla_\theta f(\theta_t + \gamma v_t) \tag{2.31}$$

$$\theta_{t+1} = \theta_t + v_{t+1} \tag{2.32}$$

The difference is that Nesterov's momentum compute the gradient in an partial updated version of the current solution $\theta_t + \gamma v_t$. [32] found that this allows NAG to change v in a more responsive way, hence gaining more stability with respect to classical momentum.

It's worth noticing that NAG is typically used in batch gradient descend, i.e not in a stochastic context, and, for this reason it's use has been often discouraged, however [32] found it to be beneficial, especially in the early stages of training, when far from convergence.

The second important factor, without which momentum is ineffective, is a proper initialization of the recurrent weight matrix. In [32] an Echo-State-Network inspired technique is used (see section 2.2.3). The idea is that the spectral radius of the weight matrix plays an important role in the dynamics of the network especially regarding memory: a too large value causes instability, where a too small one results in short memory. The founding of [32] is that the value of 1.1 is often effective.

In [32] is argued that, the way Martens's hessian-free initialize conjugate gradient (CG) , i.e using the solution found at the previous call of CG, for the quadratic minimization is a sort of hybrid NAG.

2.2.5 Dropout

Dropout was introduced in 2013 by Srivastava et al. [31] as a regularization technique for FFNNs. It does not address the vanishing/exploding gradient problem

directly and we don't know of any work which analyze the effect of dropout on memory; we report this technique nonetheless because of it's beneficial effect against over-fitting.

The idea of dropout is essentially to use ensemble learning, i.e combining the predictions of several models. In the case of FFNNs however training different models, with different data or different parameter is too computationally expensive both during training and test phases. The proposed technique is a way of approximately combining exponentially many different neural network architectures efficiently. In this context *different architectures* as to be understood as architectures with different connections between their units. This is achieved by *dropping* units, i.e temporarily removing some units from the network along with their input and output connection, with a given probability p. Applying dropout to a network results in a "thinned" version of the former. From fully connected network with n units can be derived 2^n differently thinned down networks.

At training time dropout consists in, for each example in the training batch, randomly generating a thinned down version of the original fully connected one, dropping some units, and then back-propagating the gradient to compute the update value. Note that the the update is done on the weights of the original fully connected network which are "shared" with thinned down ones; of course weights belonging to dropped-out units are not updated. Formally:

$$\boldsymbol{r} \sim Bernoulli(p) \tag{2.33}$$

$$\boldsymbol{a}^i \triangleq W^{i-1} \cdot \boldsymbol{h}^{i-1} + \boldsymbol{b}^i \qquad i = 2, ..., U \tag{2.34}$$

$$\tilde{\boldsymbol{a}}^i \triangleq \boldsymbol{a}^i \odot \boldsymbol{r} \qquad i = 2, ..., U \tag{2.35}$$

$$\boldsymbol{h}^i \triangleq \sigma(\tilde{\boldsymbol{a}}^i), \qquad i = 2, ..., U \tag{2.36}$$

$$\boldsymbol{h}^1 \triangleq \boldsymbol{x} \tag{2.37}$$

$$\boldsymbol{y} = F(\boldsymbol{a}^U) \tag{2.38}$$

where $\odot$ is the element-wise product.

At test time the original fully connected network is used, but it's weight scaled down as $W^i = pW^i$. The prediction can be viewed as a sort of average of the prediction of all the thinned down versions of the original network. The

parameter p control the amount of "noise" that is added to network, and can be tuned using a validation set.

Tough dropout has been shown [31] to improve the performance of FFNNs in several challenging tasks, it does not, as argued in [1], at least in the standard version, work well with RNNs because the recurrence amplifies too much the noise introduced by dropout. This result is in accord with the view of an RNN as a turing machine, as discussed in section 1.7; dropping units can be thought of as "corrupting" the variables of the program which implements the algorithm. A recent work by Zaremba et al., however, shows that dropout can be efficient even, with RNNs, if applied only to the non recurrent connections [35].

Chapter 3

A new SGD approach for training RNNs

Our approach for training RNNs is based entirely on the SGD framework described in Section 1.5. In particular we focus, separately, on the three main components of the algorithm, namely the initialization, the choice of the descent direction and the learning rate. We show that the initialization plays a crucial role in the learning process and can, alone, dictate if the learning process will be "successful"[1] or not. We then propose a strategy to choose a descent direction to handle with the vanishing gradient. As for the learning rate, we use a technique which is entirely equivalent to the gradient clipping trick proposed in [24] which helps dealing with exploding gradients.

3.1 Preliminaries

Before focusing on each of the three above mentioned components we will introduce some notation needed in the following sections, as well as two artificial tasks which we will use as examples. Recall from Section 1.3 that each time step is associated with a loss function. It could be zero for all time steps but for the last, for example if we want to classify the whole sequences, or it could be defined for all the time steps if each intermediate output is relevant. Consider

[1] Here we refer to artificial tasks where a criterion for success is easily defined.

now a loss function g for a generic time step τ. Defining

$$\nabla_{W_{rec}} g_{|k} \triangleq \frac{\partial g}{\partial \boldsymbol{a}^\tau} \cdot \frac{\partial \boldsymbol{a}^\tau}{\partial \boldsymbol{a}^k} \cdot \frac{\partial^+ \boldsymbol{a}^k}{\partial W^{rec}}, \tag{3.1}$$

and recalling the results of Section 1.3.2, we have

$$\frac{\partial g_\tau}{\partial W^{rec}} = \sum_{k=1}^{\tau} \nabla_{W_{rec}} g_{|k}. \tag{3.2}$$

Same definition applies for $\boldsymbol{b}_{rec}$ and W_{in}. For W_{out} (and in an analogous way $\boldsymbol{b}_{out}$) we put

$$\nabla_{W_{out}} g_{|k} \triangleq \frac{\partial g}{\partial \boldsymbol{z}^\tau} \cdot \frac{\partial^+ \boldsymbol{z}^k}{\partial W^{out}}. \tag{3.3}$$

We refer to $\nabla_{\boldsymbol{x}} g_{|k}$ as the temporal gradient for time step k w.r.t. the variable $\boldsymbol{x}$, and it is easy to see that it is the gradient computed if we would replicate the variable $\boldsymbol{x}$ and take the derivatives w.r.t. to its k-th replicate.

The **vanishing gradient** problem appears then, under this new notation, when the norm of the temporal components $\nabla_{\boldsymbol{x}} g_{|k}$ of recent time steps are exponentially bigger than the ones of more distant ones.

The two tasks, designed to enhance the vanishing gradient problem, which we will use in the following are the *addition* and the *temporal order* tasks. They belong to a set tasks proposed by Hochreiter [11] in 1991 and used as benchmarks ever since (see appendix B for more details).

The Addition task. The input sequence is composed by an $\mathbb{R}^2$ vector. The first position is a marker which can be 0 or 1 and the second position is a real number in $(0, 1)$. The goal is to predict the sum of the only two numbers marked with 1. The task is difficult because such markers are placed one at the beginning and one at the end of very long sequences.

marker	0	1	0	...	0	1	0	0
value	0.3	**0.7**	0.1	...	0.2	**0.4**	0.6	0.9

Table 3.1: An example for the addition task. The predicted output should be the sum (1.1) of the two one-marked positions.

The Temporal order task The input sequence is composed of repetitions of six different symbols $\{a, b, c, d, x, y\}$. There are only two $\{x, y\}$ symbols in the entire sequence. The goal of this task is to predict the relative order of such symbols, i.e. $\{xx, xy, yx, yy\}$, which as in the addition task, are one at the beginning and one at the end of the sequence.

3.2 Initialization

The first phase of the learning process is the initialization of the variables. We found that the choice of the initial value for the recurrent matrix W_{rec} has a big impact on the entire learning process. Recall the results from Section 1.6, where we saw that having such a matrix with too small singular values, more precisely $\sigma'_{max} \cdot \mu_{max} < 1$, is a sufficient condition for the gradient to vanish. Although a sufficient condition that, instead, guarantees that the gradient does not vanish is not known, the bounds on the singular values encourage to explore initialization techniques which lead to matrices with higher singular values or higher spectral radius. A similar suggestion, motivated by other considerations, was given in the ESN field [16].

We propose an initialization scheme where the recurrent matrix is firstly sampled from a distribution[2] and then scaled to have a specified spectral radius as shown in 3.1.

Algorithm 3.1: Recurrent weight matrix initialization scheme

Data:
ρ = desired spectral radius

1 $W_{rec} \sim \mathcal{N}(0, \sigma^2)$
2 $r \leftarrow \text{spectral\_radius}(W_{rec})$
3 $W_{rec} \leftarrow \frac{\rho}{r} \cdot W_{rec}$
4 **return** W_{rec}

In Figure 3.1 we show, as an example, the temporal gradients, w.r.t. all the variables of the model, varying the spectral radius in [0.8, 0.9, 1, 1.1, 1.2], computed on a hundred samples for the temporal order task.

The first two cases, the one with spectral radius less than one, are perfect

[2] In all the experiments we always sampled from a zero mean Gaussian, but others distributions can be used as well.

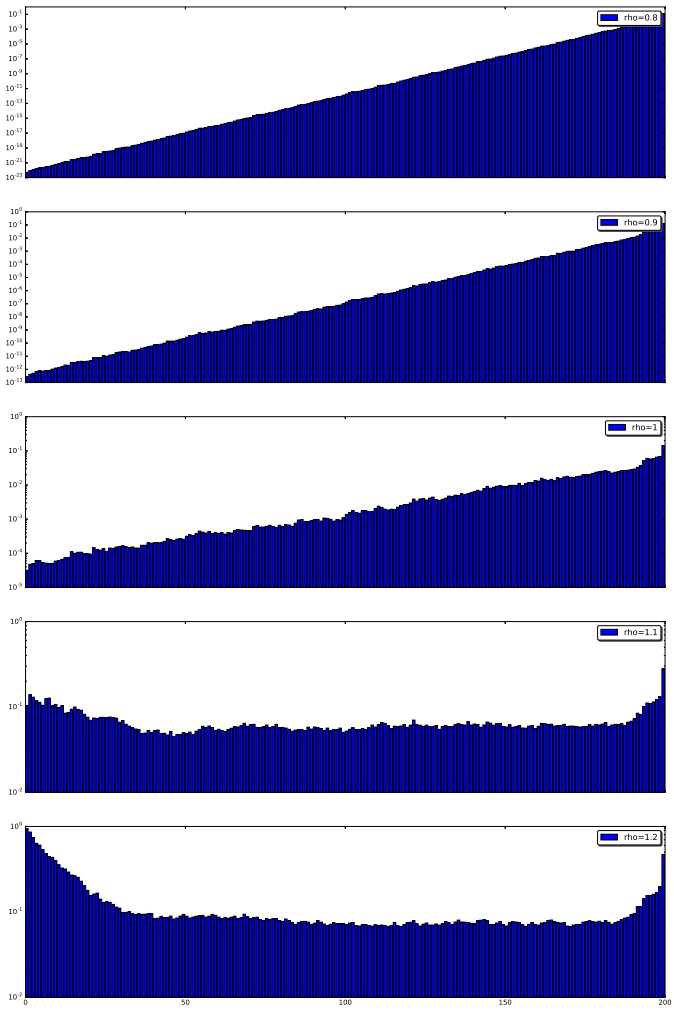

Figure 3.1: Temporal gradients for the temporal order task varying the spectral radius of the recurrent matrix. y axis is in logarithmic scale.

examples of vanishing gradient instances: more recent temporal components have norm exponentially larger than the more distant ones (please note that the y axis is in logarithmic scale). On the contrary such phenomenon is not observed in the cases of spectral radius larger than one where the temporal components have roughly the same norm.

We found that, at least in the task we explored, an appropriate spectral radius always allows the training process to start in a regime where the gradient does not vanish. We report some results on the effect of the initialization on the training process in Chapter 4.

3.3 Descent direction

In the previous section we have seen how providing a proper initialization of the recurrent matrix can lead to a starting point where gradient does not vanish. However, no matter how we choose the starting point, we have no guarantees that the gradient will not vanish after some iterations. In Figures 3.2 and 3.3, we compare the temporal gradients of two different tasks (the addition and the temporal order ones) at the beginning and after a few iterations. We notice that, although they have comparable temporal gradients norms at the beginning, they behave very differently after a few iterations: in the case of the addition task we can surely say that after a few iterations the gradient start to vanish.

Motivated by this, we introduce a new descent direction, which we will call the *simplex direction*, which should not suffer from the vanishing problem. In the following we will consider only the case where there is a single loss function L on the last time step, as in the artificial tasks, but the approach is easily generalizable to problems where a loss function is defined also for the intermediate time steps. The simplex direction is obtained by the following steps:

- Normalize the temporal gradients:

$$g_t(\boldsymbol{x}) = \frac{\nabla L_{|t}(\boldsymbol{x})}{\left\|\nabla L_{|t}(\boldsymbol{x})\right\|}. \tag{3.4}$$

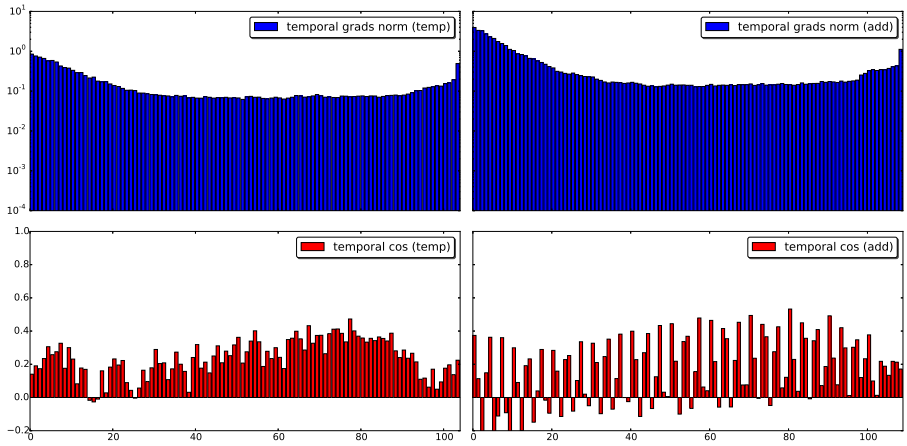

Figure 3.2: Comparison between the temporal order task (first column) and the addition task (second column). First row shows the norms of the temporal gradients, while the second shows the cosine between each temporal component and the gradient. This is a snapshot taken at the first iteration of the training process.

- Combine the normalized gradients in a convex way:

$$g(\boldsymbol{x}) = \sum_{t=1}^{T} \beta_t \cdot g_t(\boldsymbol{x}). \tag{3.5}$$

  with $\sum_{t=1}^{T} \beta_t = 1, \beta_t > 0$ (randomly picked at each iteration).

- Introduce the gradient norm:

$$d(\boldsymbol{x}) = - \|\nabla L(\boldsymbol{x})\| \frac{g(\boldsymbol{x})}{\|g(\boldsymbol{x})\|}. \tag{3.6}$$

As we have seen in Section 1.3.2 the anti-gradient direction is the sum of all temporal gradients. The idea is to combine the gradients in such a way that the gradient contains information about all time steps, i.e. does not suffer from the vanishing problem. This is achieved by normalizing all the temporal gradients. The idea to combine them in a convex, simplex-type way, as suggested by some numerical evidence, adds some robustness to the method. Finally since we discard any information about the norms in the normalization process, we choose to give the simplex direction the norm of the gradient. In this way we can see the obtained direction as a projection of the gradient.

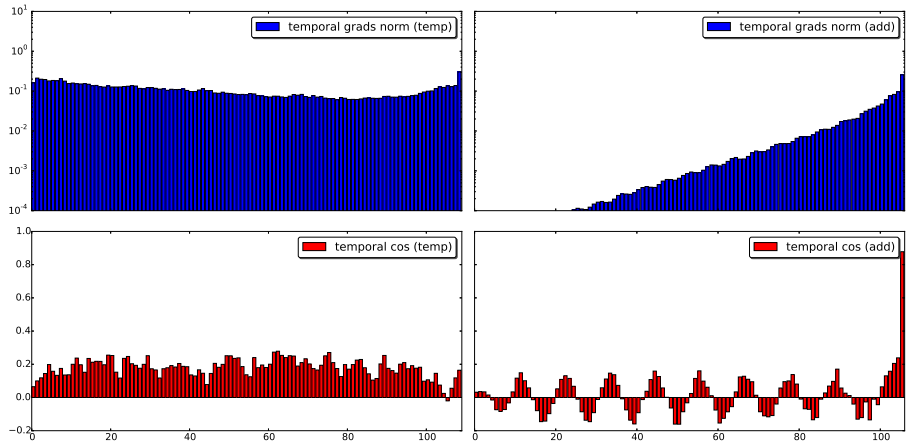

Figure 3.3: Caption as in Figure 3.2. This is a snapshot taken after a few iterations of the training process.

3.4 Learning rate

The choice of the learning rate is crucial for the success of the training procedure. It is well known that RNNs give rise to gradients which change extremely fast in norm (the exploding gradient problem). This makes choosing a single constant step, or even designing an adaptive strategy, very difficult, at the least, for this kind of models. A simple trick which allow to choose a fixed step from the beginning is to *clip the gradients*. This technique was introduced and used in slightly different forms in [24] and [20] and we described it in Section 2.2.1. We reformulate the version proposed in [24] as a learning rate selection strategy. Given a direction $\boldsymbol{d}_k$ the step α_k is chosen as:

$$\alpha_k = \begin{cases} \mu & \text{if } \|\boldsymbol{d}_k\|_2 \leq \tau \\ \frac{\mu \cdot \tau}{\|\boldsymbol{d}_k\|_2} & otherwise, \end{cases} \tag{3.7}$$

where μ and c are some positive constants. The parameter τ is the threshold on the direction norm; μ, instead, is the constant learning rate that is used when the norm of the direction is not above such threshold. The idea is to use a constant step when the direction has small enough norm and vice-versa choose a step which is inversely proportional when such norm is too large. We confirm, as found in works cited above, that this trick is essential to train RNNs in a

stochastic framework.

3.5 Putting all together

Now that we have described all the three main components of the algorithm we can put them together, as we do in Algorithm 3.2, but with an important additional feature. The idea is to use the simplex combination at the beginning of the training process, or whenever the gradient is vanishing, and switch back to the anti-gradient when appropriate. This is done by checking the norm of the gradient, as in Line 12.

Algorithm 3.2: RNN training

Data:
$D = \{\langle \boldsymbol{x}^{(i)}, \boldsymbol{y}^{(i)} \rangle\}$: training set
m: size of each mini-batch
μ: constant learning rate
τ: gradient clipping threshold
ρ: initial spectral radius
ψ threshold for the direction norm

Result:
θ: solution

1 $W_{rec}, W_{in}, W_{out} \sim \mathcal{N}(0, \sigma^2)$
2 $\boldsymbol{b}_{out}, \boldsymbol{b}_{rec} \leftarrow 0$
3 $r \leftarrow \text{spectral\_radius}(W_{rec})$
4 $W_{rec} \leftarrow \frac{\rho}{r} \cdot W_{rec}$
5 $\theta_0 = [W_{rec}, W_{in}, W_{out}, \boldsymbol{b}_{out}, \boldsymbol{b}_{rec}]$
6 **while** *stop criterion* **do**
7 $I \leftarrow$ sample m training example $\in D$
8 $\{\nabla_\theta L_{|t}\}_{t=1}^{T} \leftarrow \text{compute\_temporal\_gradients}(\theta_k, I)$
`/* T is the length of the sequences. All sequences in a batch have the same length */`
9 $\boldsymbol{d}_k \leftarrow \text{simplex\_combination}(\{\nabla_\theta L_{|t}\})$
10 $\alpha \leftarrow$ compute learning rate
11 **if** $\|\nabla_\theta L(\theta_k)\|_2 > \psi$ **then**
12 $\boldsymbol{d}_k \leftarrow \nabla_\theta L(\theta_k)$
13 **end**
14 $\alpha_k = \begin{cases} \mu & \text{if } \|\boldsymbol{d}_k\|_2 \leq \tau \\ \frac{\mu \cdot \tau}{\|\boldsymbol{d}_k\|_2} & \text{otherwise} \end{cases}$
15 $\theta_{k+1} \leftarrow \theta_k + \alpha_k \boldsymbol{d}_k$
16 $k \leftarrow k + 1$
17 **end**
18 **return** θ_k

3.6 Proof of convergence

In this section we demonstrate that, under favorable assumptions, convexity among them, a closely related version of our SGD exhibit some kind of convergences properties. This should help understand and motivate our work, in particular why picking a descent direction different from the anti-gradient works. It is important to note that RNNs give rise to non-convex function, even when the loss function is convex, so this proof is not directly applicable, in any case, to our scenario. We start from the work of Nemirowski et al. [22] and modify their proof of convergence. In here we report all of the proof for sake of completeness, but our contribution is limited to equations (3.20) - (3.24) and (3.32) - (3.36).

Consider the stochastic optimization problem

$$\min_{\boldsymbol{x}\in\mathbb{R}^n} f(\boldsymbol{x}) = \mathbb{E}[\mathbb{F}(\boldsymbol{x}, \boldsymbol{\xi})], \tag{3.8}$$

where $\boldsymbol{\xi} \in \Omega \subset \mathbb{R}^d$ is a random vector. Suppose $f(\cdot)$ is continuous, strongly convex (with constant c) and there exists a compact level set of $f(\cdot)$, hence (3.8) has a unique optimal solution $\boldsymbol{x}_*$. We make the following two assumptions:

- It is possible to generate independent identically distributed samples of $\boldsymbol{\xi}$.
- There exists an oracle which, for a given point $(\boldsymbol{x}, \boldsymbol{\xi})$ returns a stochastic direction $D(\boldsymbol{x}, \boldsymbol{\xi})$ such that $d(\boldsymbol{x}) \triangleq \mathbb{E}[D(\boldsymbol{x}, \boldsymbol{\xi})]$ satisfies:

$$-(\boldsymbol{x} - \boldsymbol{x}_*)^T(f' - d(\boldsymbol{x})) \geq -\mu L \|\boldsymbol{x} - \boldsymbol{x}_*\|_2^2 \quad \text{for some } f' \in \partial f(\boldsymbol{x}), \tag{3.9}$$

  for some $\mu \in (0, \frac{c}{L})$, L is some chosen positive constant. We assume further that there exists $M > 0$ such that

$$\|d(\boldsymbol{x})\|_2^2] \leq M^2 \quad \forall \boldsymbol{x} \in \mathbb{R}^n. \tag{3.10}$$

Consider an algorithm defined by

$$\boldsymbol{x}_{j+1} = \boldsymbol{x}_j - \gamma_j D(\boldsymbol{x}_j, \boldsymbol{\xi}_j). \tag{3.11}$$

Each iterate $\boldsymbol{x}_j$ of such a random process is a function of the history $\boldsymbol{\xi}_{[j-1]} =$

$(\boldsymbol{\xi}_1, \ldots, \boldsymbol{\xi}_{j-1})$.

Let $A_j \triangleq \|\boldsymbol{x}_j - \boldsymbol{x}_*\|_2^2$ and $a_j \triangleq \mathbb{E}[A_j]$. From (3.11) we get

$$\begin{aligned} A_{j+1} &= \frac{1}{2}\left\|\boldsymbol{x}_j - \gamma_j D(\boldsymbol{x}_j, \boldsymbol{\xi}_j) - \boldsymbol{x}_*\right\|_2^2 \\ &= A_j + \frac{1}{2}\gamma_j^2 \left\|D(\boldsymbol{x}_j, \boldsymbol{\xi}_j)\right\|_2^2 - \gamma_j (\boldsymbol{x}_j - \boldsymbol{x}_*)^T D(\boldsymbol{x}_j, \boldsymbol{\xi}_j). \end{aligned} \tag{3.12}$$

We can write:

$$\mathbb{E}_{\boldsymbol{\xi}_{[j]}}[(\boldsymbol{x}_j - \boldsymbol{x}_*)^T D(\boldsymbol{x}_j, \boldsymbol{\xi}_j)] = \mathbb{E}_{\boldsymbol{\xi}_{[j-1]}}[\mathbb{E}_{\boldsymbol{\xi}_{[j]}}[(\boldsymbol{x}_j - \boldsymbol{x}_*)^T D(\boldsymbol{x}_j, \boldsymbol{\xi}_j)]|\boldsymbol{\xi}_{[j-1]}] \tag{3.13}$$

$$= \mathbb{E}_{\boldsymbol{\xi}_{[j-1]}}[(\boldsymbol{x}_j - \boldsymbol{x}_*)^T \mathbb{E}_{\boldsymbol{\xi}_{[j]}}[D(\boldsymbol{x}_j, \boldsymbol{\xi}_j)]|\boldsymbol{\xi}_{[j-1]}] \tag{3.14}$$

$$= \mathbb{E}_{\boldsymbol{\xi}_{[j-1]}}[(\boldsymbol{x}_j - \boldsymbol{x}_*)^T d(\boldsymbol{x}_j)]. \tag{3.15}$$

Equation (3.13) is given by the law of total expectation, (3.14) holds because $\boldsymbol{x}_j = \boldsymbol{x}_j(\boldsymbol{\xi}_{[\boldsymbol{j-1}]})$ is not function of $\boldsymbol{\xi}_j$, hence independent of it. Using (3.10) and (3.15) we obtain, taking expectation on both sides of (3.12),

$$a_{j+1} \leq a_j - \gamma_j \mathbb{E}_{\boldsymbol{\xi}_{[j-1]}}[(\boldsymbol{x}_j - \boldsymbol{x}_*)^T d(\boldsymbol{x}_j)] + \frac{1}{2}\gamma_j^2 M^2. \tag{3.16}$$

Since $f(\cdot)$ is strongly convex with constant $c > 0$,

$$(\boldsymbol{x} - \boldsymbol{y})^T (f' - g')) \geq c\|\boldsymbol{x} - \boldsymbol{y}\|_2^2, \quad \forall f' \in \partial f(\boldsymbol{x}), g' \in \partial f(\boldsymbol{y}). \tag{3.17}$$

By optimality of $\boldsymbol{x}_*$ we have

$$(\boldsymbol{x} - \boldsymbol{x}_*)^T f' \geq 0 \quad \forall \boldsymbol{x} \in \mathbb{R}^n, \forall f' \in \partial f(\boldsymbol{x}_*). \tag{3.18}$$

Inequalities (3.17) and (3.18) together imply

$$(\boldsymbol{x} - \boldsymbol{x}_*)^T f' \geq c\|\boldsymbol{x} - \boldsymbol{x}_*\|_2^2 \quad \forall \boldsymbol{x} \in \mathbb{R}^n, \forall f' \in \partial f(\boldsymbol{x}). \tag{3.19}$$

Adding and subtracting the oracle direction $d(\boldsymbol{x})$ we get

$$(\boldsymbol{x} - \boldsymbol{x}_*)^T (f' - d(\boldsymbol{x}) + d(\boldsymbol{x})) \geq c\|\boldsymbol{x} - \boldsymbol{x}_*\|_2^2, \tag{3.20}$$

which can be rewritten as

$$(\boldsymbol{x} - \boldsymbol{x}_*)^T d(\boldsymbol{x}) \geq c \left\| \boldsymbol{x} - \boldsymbol{x}_* \right\|_2^2 - (\boldsymbol{x} - \boldsymbol{x}_*)^T (f' - d(\boldsymbol{x})). \tag{3.21}$$

From Assumption (3.9), and by taking expectations (from now on we will write $\mathbb{E}$ in place of $\mathbb{E}_{\boldsymbol{\xi}_{[j-1]}}$ for ease of notation) on both side of (3.21), we obtain

$$\mathbb{E}[(\boldsymbol{x}_j - \boldsymbol{x}_*)^T (\boldsymbol{x}_j)] \geq c\mathbb{E}[\|\boldsymbol{x}_j - \boldsymbol{x}_*\|_2^2)] - \mathbb{E}[(\boldsymbol{x}_j - \boldsymbol{x}_*)^T (f_j' - d(\boldsymbol{x}_j))] \tag{3.22}$$

$$\geq c \left(1 - \frac{\mu L}{c}\right) \mathbb{E}[\|\boldsymbol{x}_j - \boldsymbol{x}_*\|_2^2] \tag{3.23}$$

$$= 2\bar{c} a_j, \tag{3.24}$$

with $\bar{c} = c(1 - \frac{\mu L}{c})$ and $f_j' \in \partial f(\boldsymbol{x}_j)$. Hence from (3.16) it follows

$$a_{j+1} \leq (1 - 2\bar{c}\gamma_j) a_j + \frac{1}{2} \gamma_j^2 M^2. \tag{3.25}$$

Choosing now the stepsizes as $\gamma_j = \frac{\beta}{j}$ for some constant $\beta > \frac{1}{2\bar{c}}$ we get

$$a_{j+1} \leq (1 - 2\bar{c}\gamma_j) a_j + \frac{1}{2} \frac{\beta^2 M^2}{j^2}. \tag{3.26}$$

It follows by induction that

$$\mathbb{E}[\|\boldsymbol{x}_j - \boldsymbol{x}_*\|_2^2] = 2a_j \leq \frac{Q(\beta)}{j}, \tag{3.27}$$

where

$$Q(\beta) = \max \left\{ \frac{\beta^2 M^2}{2\bar{c} - 1}, \|\boldsymbol{x}_1 - \boldsymbol{x}_*\|_2^2 \right\}. \tag{3.28}$$

When ∇f is Lipschitz continuous we also have

$$f(\boldsymbol{x}) \leq f(\boldsymbol{x}_*) + \frac{1}{2} L \left\| \boldsymbol{x} - \boldsymbol{x}_* \right\|_2^2, \quad \forall \boldsymbol{x} \in \mathbb{R}^n, \tag{3.29}$$

hence we can get a bound also on the function value:

$$\mathbb{E}[f(\boldsymbol{x}_j) - f(\boldsymbol{x}_*)] \leq \frac{1}{2} L \, \mathbb{E}[\|\boldsymbol{x}_j - \boldsymbol{x}_*\|_2^2] \leq \frac{1}{2} L \, Q(\beta). \tag{3.30}$$

Assumption (3.9) can be further elaborated. Let θ be the angle between

$f' \in \partial f(\boldsymbol{x})$ and $d(\boldsymbol{x})$. Write $\|d(\boldsymbol{x}_j)\| = \alpha \|\nabla f(\boldsymbol{x}_j)\|$ for some $\alpha > 0$, then

$$\|f' - d(\boldsymbol{x}_j)\|^2 = \|f'\|^2 + \|d(\boldsymbol{x}_j)\|^2 - 2\|f'\| \|d(\boldsymbol{x}_j)\| \cos\theta_j \tag{3.31}$$

$$= \|f'\|^2 (1 + \alpha_j^2 - 2\alpha_j \cos\theta_j). \tag{3.32}$$

Hence

$$(\boldsymbol{x} - \boldsymbol{x}_*)^T (f' - d(\boldsymbol{x})) \leq \|\boldsymbol{x} - \boldsymbol{x}_*\| \|f' - d(\boldsymbol{x})\| \tag{3.33}$$

$$= \|\boldsymbol{x} - \boldsymbol{x}_*\| \|f'\| (1 + \alpha_j^2 - 2\alpha_j \cos\theta_j)^{\frac{1}{2}} \tag{3.34}$$

Assume

$$\|f'\|_2 \leq L \|\boldsymbol{x} - \boldsymbol{x}_*\|_2 . \tag{3.35}$$

Note that Equation (3.35) is implied simply by Lipschitz continuity in the differentiable case. A sufficient condition is thus

$$1 + \alpha^2 - 2\alpha \cos\theta_j \leq \left(\frac{\mu}{L}\right)^2 . \tag{3.36}$$

Chapter 4

Numerical experiments

4.1 Experiments on synthetic datasets

In this section we report some numerical experiments to highlight the effects of the proposed techniques on the training process. In all the experiments with artificial dataset we employed a potentially infinite training-set, since we generate data on the fly. We used a validation set to determine the success of the training process. We define a training run to be successful if the error on the validation set if less than 1%. The error is clearly defined for each task, see Appendix B for more details on the tasks. We say a run as unsuccessful is the loss do not decrease for more than $3 \cdot 10^6$ iterations. The validation test is composed by 10^4 examples of different lengths sampled once at the beginning. In all the experiments we used RNNs with 50 hidden units trained with a learning rate of 10^{-3}, clipping threshold of 1, batch size equal to 100, initial spectral radius of 1.2. We did not experiment much on the batch size. We found instead that the this combination of learning rate and threshold is generally good for all the task and lengths, although for tasks with smaller sequences more aggressive learning rate can be used.

4.1.1 The effect of the spectral initialization

For this experiment we consider the temporal order task which has always been considered effectively impossible to solve using a plain version of the stochastic

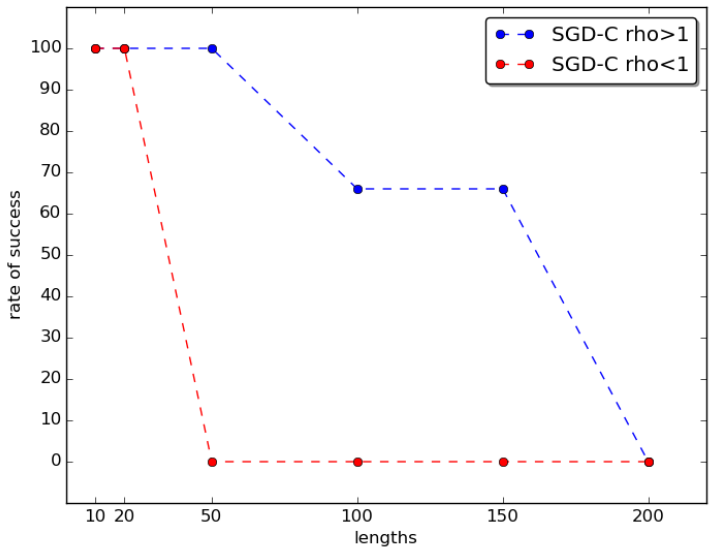

Figure 4.1: Rate of success (mean of 5 runs) for the temporal order task for various lengths with SGD modified with gradient clipping. In blue and red the results when W_{rec} is initialized with spectral radius bigger and smaller than one respectively.

gradient descent algorithm. In [2], for instance, are reported the rate of success of SGD and SGD modified with gradient clipping technique for such a task with different input lengths. It shows that for sequences longer than 20 neither one of the algorithms can solve the problem. We repeated the same experiment, namely training the network varying the length[1] of the input sequences, with the SGD algorithm modified with the gradient clipping technique (SGD-C) using our initialization scheme.

In Figure 4.1 we compare the rate of success between an initialization scheme using only a standard Gaussian initialization, and the initialization scheme by us proposed where W_{rec} is scaled to have spectral radius larger than one. We notice that scaling the recurrent matrix has a huge effect on the rate of success: where the standard scheme failed for sequences longer than 20, with the spectral initialization we managed to succeed up to sequences of length 150.

[1]Here we refer as the length of the task to the minim length of the input sequences

anti-gradient	simplex	simplex with conditional switching
1807466	2338500	1630666

Table 4.1: Number of iterations until convergence for the addition task (T=100). Mean of 3 runs.

4.1.2 The effect of using the simplex direction

The first experiment we ran is developed to compare the simplex strategy and the variant with the conditional switching to the anti-gradient with the standard SGD. We tested the three algorithms on the addition problem (T=100). In Figure 4.2 is shown the loss on the validation set during the training process (until convergence).

The first part of the learning process is particularly interesting because it highlights the differences between the simplex and the anti-gradient direction in the regime of vanishing gradients. In the anti-gradient case the loss remains roughly constant for a good portion of the whole training time until it starts decreasing significantly. The other two strategies perform differently. In fact they both start decreasing a lot sooner in all the three runs. This should suggests that using the simplex direction helps the training process when the gradient is vanishing, which happens in the first part of the training.

In the second part of the training process, i.e., when the loss is decreasing, relatively rapidly, gradients do not vanish and moreover have large norm. We can see from the plots that the simplex direction can perform poorly in this second part compared to the anti-gradient one. So, the idea of switching back to the ant-gradient direction in this phase proves to be beneficial.

In Table 4.1 are shown the number of iterations (mean values of 3 runs) needed for convergence for each strategy. Notice that the simplex direction with conditional switching obtains the best result.

We repeated the experiment also for the temporal order task and ... ADD RESULTS WHEN READY

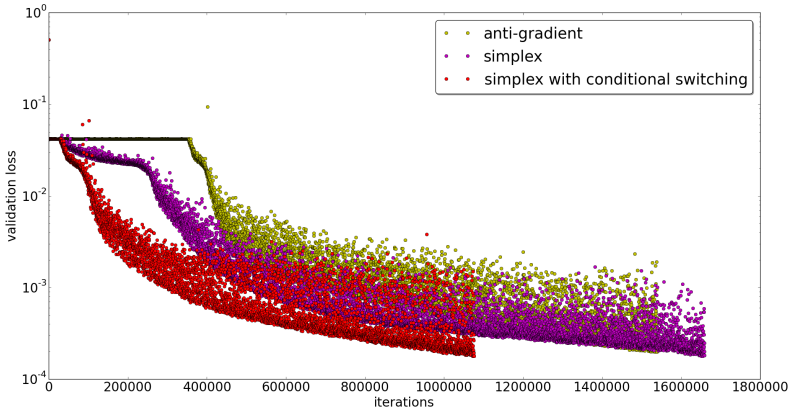

(a) First run

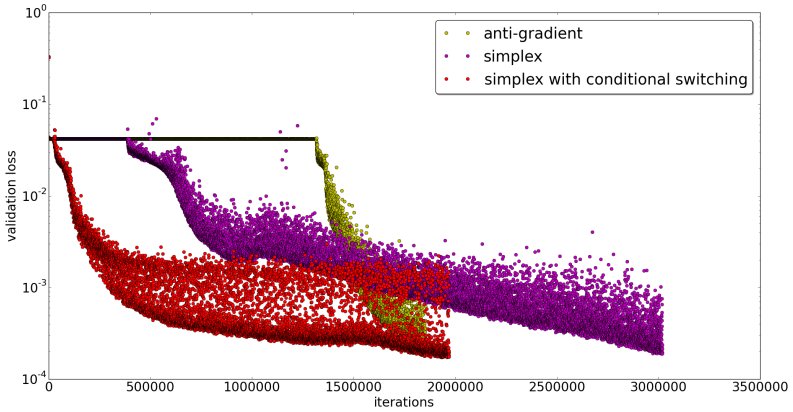

(b) Second run

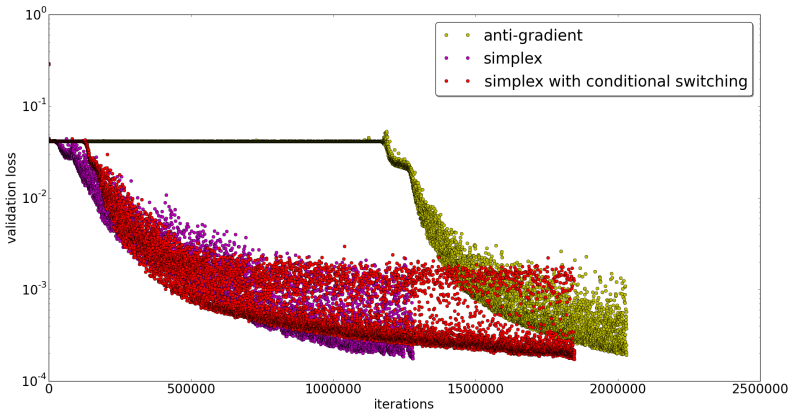

(c) Third run

Figure 4.2: Comparison between SGD using as descent direction the anti-gradient (in yellow, start decreasing always for last), the simplex direction (in purple, which is the second that start decreasing) and the simplex direction with conditional switching (in red, start decreasing always for first) for the addition task (T=100). In y axis the loss (mean squared error) in logarithmic scale.

4.2 Polyphonic music prediction

In this experiment we considered the task of polyphonic music prediction. The input sequences are polyphonic songs and the aim is, at each time step, to predict which notes are going to be played next. More precisely the input sequences are obtained from a piano roll of MIDI files where each time step corresponds to a beat (usually a quarter or an octave): each step of the sequence is hence composed of d binary elements which specify if the correspondent note is played or not at the current beat, where d is the number of notes that can be played.

We use as a reference the work done in [5] which compares several different approaches, RNNs amongst them. We use the dataset *MuseData* made available by the authors on their website `http://www-etud.iro.umontreal.ca/~boulanni/icml2012`, using the provided split in train, set and validation sets.

The RNN architecture we employed is a standard RNN with *tanh* units, 88 input and output units (the total number of notes from A0 to C8). We use as output function the logistic function

$$F(x) = \frac{1}{1 + e^{-x}}. \tag{4.1}$$

In this way we can interpret the value of each output unit as the probability that such note is played, as for each note we have an output in $(0, 1)$. We used the cross-entropy as loss function for each time step, hence, the loss for the whole sequence is given by:

$$L(\boldsymbol{y}) = \frac{1}{T} \sum_{t=1}^{T} \sum_{i=1}^{d} \bar{y}_i^t \log(y_i^t) + (1 - \bar{y}_i^t) \log(1 - y_i^t), \tag{4.2}$$

where, as usual, y_i^t and $\bar{y}_i^t$ are the predicted output and the label for note i at time t respectively.

An important difference compared to the artificial tasks considered before is that in this case the loss is not computed only on the last step. This has, of course, an impact on the temporal gradients as the gradient seems not to vanish in this scenario.

We trained the network with SGD (with the anti-gradient direction) with learning rate 0.001 and threshold on the gradient norm 3. We explored different

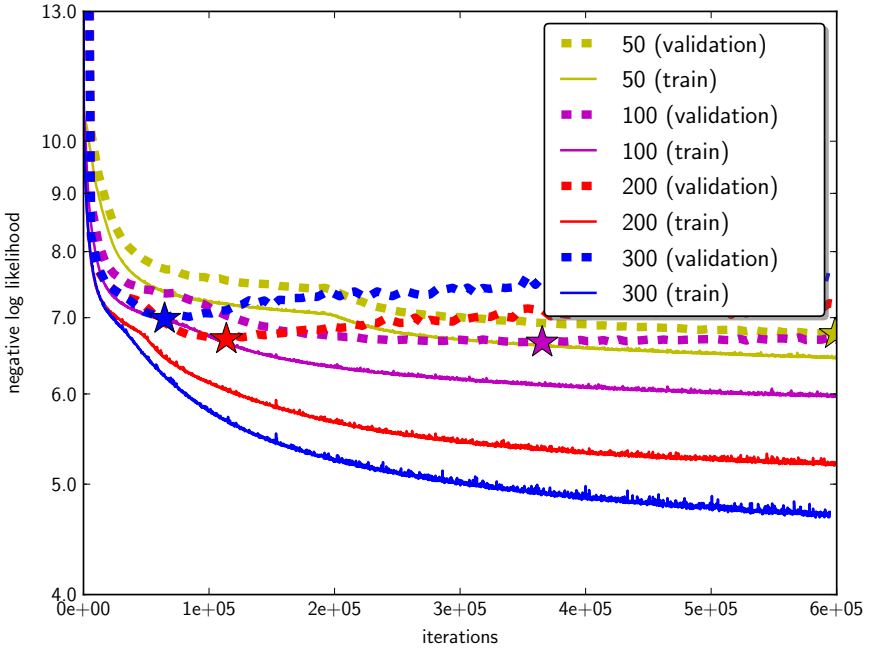

Figure 4.3: Loss on both train and validation sets during training for models with different number of hidden units. The stars mark the best values on the validation sets.

number of hidden units, namely 50, 100, 200, 300. We compose the batch with sequences of different lengths, up to 300 steps, cutting the original songs if they are longer than 300 steps.

Figure 4.3 shows the loss function computed on both train and validation sets during the training for model with different hidden units. The most obvious observation is that at a certain point the training procedure starts to over-fit and that the model with more hidden units start to over-fit sooner.

In Table 4.3 the test and train error for state of art approaches as well as

hidden units	test loss	train loss
50	**6.44**	6.20
100	6.53	6.10
200	6.58	**6.03**
300	6.82	6.21

Table 4.2: This table shows the loss (i.e. negative log-likelihood per time step) for both train and test sets for the models with different number of hidden units.

	State of art (RNN-NADE)	State of art for vanilla RNN	Our result
Train	**5.20**	6.43	6.20
Test	**5.60**	6.97	6.44

Table 4.3: Comparison between test and train errors with state of art results.

our as shown. Although our result is worse than the state of the art, which is held by RNN-NADE [5] trained with HF optimization, we improve the best result obtained with vanilla RNNs. The reason for this (partial) success can be attributed to the choice of the hyper-parameters or the way we build up the batches.

4.3 Lupus disease prediction

This experiment involves real data gathered by "Lupus Clinic", Reumatologia, Università Sapienza, Roma. The data consists in 413 patients. It is available the records of the visits that every patience has done over time. For an in-depth description of the data we refer the reader to the work of Francesco Morelli, that served as starting point of our work. In his thesis, "Tecniche di apprendimento automatico per la classificazione di pazienti affetti da Lupus", he performed an analysis of the data which does not take into account the history of the patience: only the first visit of each patience is considered with the aim to classify a patience as affected or unaffected by the disease at the time of the visit. This analysis led also to the identification of a subset[2] of features which appear to be the most relevant for the prediction. Our goal is slightly different: we aim to predict whether a patience will develop the lupus disease before it is evident from organic damage, i.e. when the SDI (systemic damage index) is zero). This is done considering not only the first visit of a patience but his complete history.

For the purpose of this thesis, the important things to underline are essentially two. The first one is that, although each visit is described by a fixed number real and binary features, the number of visits is not the same for each

[2]The subset of selected features is [Hashimoto, APS , npsle, arterialthrombosis, MyasteniaGravis, FM, age] over the whole set [APS, DNA, FM, Hashimoto, MyasteniaGravis, SdS, age, arterialthrombosis, arthritis, c3level, c4level, dislipidemia, hcv, hematological, hypertension, hypothyroidism, kidney, mthfr, npsle, pregnancypathology, serositis, sex, skinrash, sledai2kInferred].

patience. RNNs then emerges as one of few models suitable for such a task. The other important thing to notice is that the visits are not equally spaced in time; they can be distanced by a month as by a few years. This is an important difference to all of the tasks considered until now. Let us think for example of the polyphonic music prediction where each song is split in equally spaced time beats.

In the experiments we used as **positive** examples all the patients which are negative at the first visit but results positive in later visits (i.e. we excluded completely all the patients which are positive from the first visit). We used as training sequences only the visits in which the patients has zero SDI . For the **negative** examples we choose only the patients which satisfy some temporal constraints controlled by user-defined parameters. The first requirement is for the recorded history of a patience to be long enough to be able to leave out the last part of it from the training sequence. This ensures that we train the model to give a prediction valid[3], at least, for such given amount of time. We measured this time (in years) with the parameter `upper span age`. We then require the remaining part of the visits (which are the only ones used in the training sequence) to cover a sufficiently long period of time with the parameter (in years) `lower span age` and to be composed by at least `min visits` number of visits. This last two constraints are needed to filter out the examples which do not have enough information: if the network has to understand the data from its evolution over time, we should have sufficiently many recordings for a sufficient amount of time.

We employed the following metrics to evaluate the results of the experiments:

- $precision \triangleq \frac{TP}{TP+FP}$,
- $recall(sensitivity) \triangleq \frac{TP}{P}$,
- $specificity \triangleq \frac{TN}{N}$,
- area under curve (AUC): the area under the curve obtained plotting recall and specificity varying the threshold of the classifier,

[3]Contrarily to a positive patience who cannot become negative once he has positive SDI, for negative patients there is always the possibility to result positive in the future. This suggest to restrict the prediction to a span of years and use as negatives in the training process only the patience which result negative for that period of time.

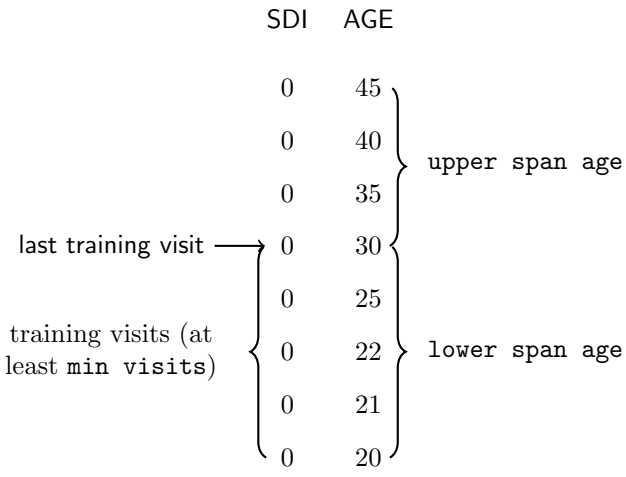

Figure 4.4: Example of a negative training sequence.

where TP, TN, P, N are the true positive, true negative, number of positive and number of negatives respectively. See [9] for more details on these metrics.

We normalized all the data to lie in range (0,1). We used RNNs with 50 hidden units trained with SGD paired with the gradient clipping technique (learning rate 0.001 and threshold 1).

Since the number of available patients is not big enough to allow a split in train, validation and test sets, each experiment was done according to the following procedure. The entire dataset is split in train e test sets, we train the model until the AUC score on the training set is below 0.92. Then we compute the predictions of the trained model on the test set. We repeat this procedure 8 times with 8 different split in train and test in such a way that all the examples are used once as test examples. We then aggregate all the predictions on the 8 different test sets to compute the final score.

We explored all the combination for `upper span age` in [1, 2], `lower span age` in [1, 2], `min visits` in [2, 3, 4, 5]. We repeated the experiment twice: on time with all the features and next with the subset of selected features.

From the results, shown in Table 4.4, seems clear that the models trained with patients with more visits result in better AUC score. The other parameters, namely `upper span age` and `lower span age`, seems to have a little bit less influence. Moreover we notice that the better results are obtained by the models trained with the selected subset of features. In Figures 4.5, 4.6 and 4.7 are shown

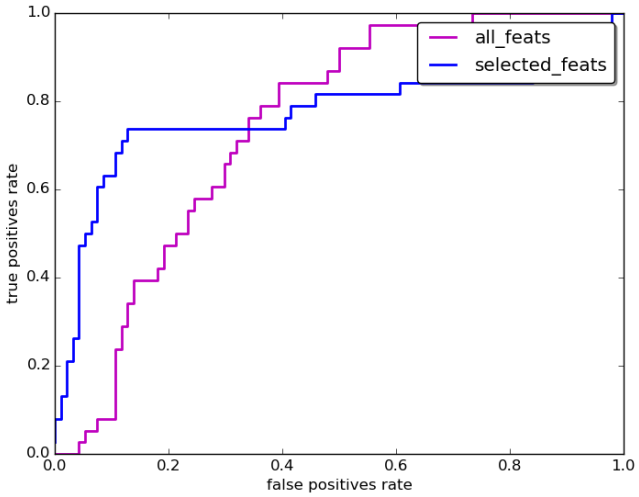

Figure 4.5: roc curve for models of Line **??** of Table 4.4.

the plots of the roc, sensitivity-specificy and recall-precision curves for the best configuration of parameters (`upper span age`=0.8, `lower span age`=0.8 and `min visits`=5).

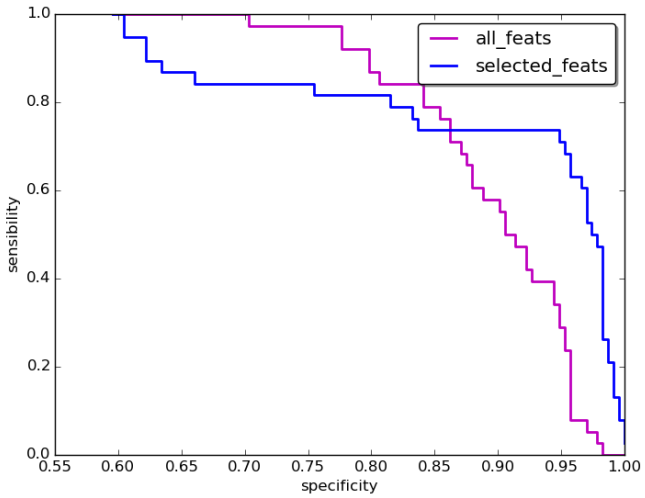

Figure 4.6: Sensitivity-specificity for models of Line **??** of Table 4.4.

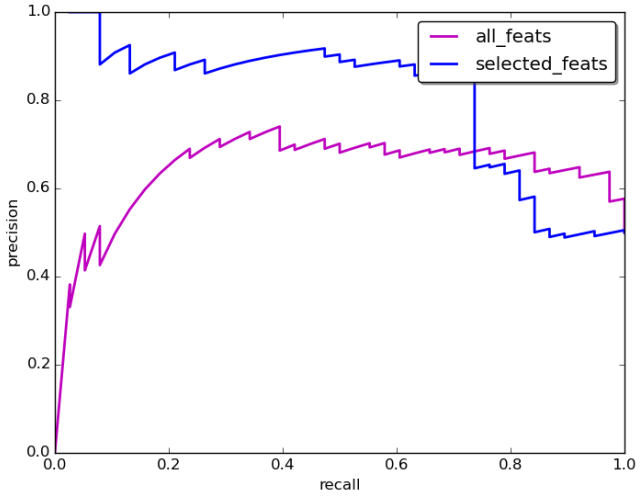

Figure 4.7: Precision-recall curve for models of Line **??** of Table 4.4.

upper span age	lower span age	min visits	AUC all feats	AUC subset feats	pos	neg
0.8	0.8	1	0.63	0.65	38	143
0.8	0.8	2	0.66	0.63	38	138
0.8	0.8	3	0.71	0.67	38	124
0.8	0.8	4	0.69	0.75	38	115
0.8	0.8	5	0.74	**0.77**	38	94
1.0	0.8	1	0.69	0.61	38	141
1.0	0.8	2	0.68	0.60	38	133
1.0	0.8	3	0.68	0.67	38	121
1.0	0.8	4	0.69	0.73	38	108
1.0	0.8	5	0.74	0.76	38	88
2.0	0.8	1	0.72	0.68	38	99
2.0	0.8	2	0.71	0.67	38	97
2.0	0.8	3	0.73	0.72	38	90
2.0	0.8	4	0.74	0.73	38	70
2.0	0.8	5	0.69	**0.77**	38	48
0.8	1.0	1	0.64	0.65	38	138
0.8	1.0	2	0.69	0.68	38	133
0.8	1.0	3	0.66	0.69	38	122
0.8	1.0	4	0.67	0.69	38	114
0.8	1.0	5	0.69	0.72	38	93
1.0	1.0	1	0.67	0.60	38	134
1.0	1.0	2	0.64	0.52	38	127
1.0	1.0	3	0.73	0.68	38	118
1.0	1.0	4	0.73	0.73	38	107
1.0	1.0	5	0.70	0.73	38	87
2.0	1.0	1	0.69	0.62	38	89
2.0	1.0	2	0.72	0.59	38	87
2.0	1.0	3	0.73	0.63	38	83
2.0	1.0	4	0.74	0.67	38	67
2.0	1.0	5	0.69	0.75	38	48
0.8	2.0	1	0.63	0.72	38	97
0.8	2.0	2	0.67	0.66	38	95
0.8	2.0	3	0.70	0.73	38	92
0.8	2.0	4	0.68	0.69	38	91
0.8	2.0	5	0.70	0.76	38	83
1.0	2.0	1	0.64	0.66	38	88
1.0	2.0	2	0.64	0.69	38	86
1.0	2.0	3	0.66	0.66	38	85
1.0	2.0	4	0.62	0.71	38	84
1.0	2.0	5	0.67	0.74	38	74
2.0	2.0	1	0.64	0.67	38	45
2.0	2.0	2	0.68	0.58	38	44
2.0	2.0	3	0.68	0.67	38	43
2.0	2.0	4	0.70	0.64	38	41
2.0	2.0	5	0.66	0.69	38	35

Table 4.4: AUC core for different training sets. Best score in bold.

Chapter 5

Conclusion

We started our analysis from the gradient structure of RNNs. We showed how the recurrent nature of this model change the gradient structure in comparison to FFNNs. In particular the recurrence definition of RNNs give rise to the *exploding/vanishing* gradient problem. We then analyzed some sufficient conditions for the gradient to vanish. In particular we found that the singular values of the recurrent matrix play an important role in the matter, namely, if the recurrent matrix has too small singular values the gradient vanish.

Motivated by this, we explored an initialization scheme which scales the recurrent matrix to have spectral radius larger than one. We showed that, with such an initialization, several artificial tasks that were deemed impossible to solve with SGD, for sequences longer than 20, can be solved with a non zero rate of success. This is particularly interesting because the proposed initialization scheme is extremely simple to implement and for several real application can be enough to obtain good results.

Furthermore we proposed a novel strategy to pick a descent direction based on a combination of what we call the temporal gradients, namely, the gradients we would obtain taking the derivatives of the replicates of each variable for each time step. TODO EFFECTS.

Finally we considered two real application. The first one is the polyphonic music prediction, where the task is, given a song, to predict at each time beat, which notes are going to be played next. The main difference with the artificial

tasks is that, in this case, there is a non zero loss for each time step. We noticed that this has a huge effect on the gradient which seems not to vanish whatever the initialization. The second application, instead, comes from the recording of medical visits of patients affected by the lupus disease. The aim here is to predict whether a patience will result affected by the disease or not in the near future. Also in this scenario, since the sequences, which consist in the visits each patience has done over time, are not longer than 20, we did not observe a vanishing gradient even if the loss is defined only on the last time step.

FUTURE WORK?

Appendix A

Notation

Let $F : \mathbb{R}^N \to \mathbb{R}^M$ be defined by

$$F(\boldsymbol{x}) = (f_1(\boldsymbol{x}), f_2(\boldsymbol{x}), \cdots, f_M(\boldsymbol{x}))) \text{ for some } f_i : \mathbb{R}^N \to \mathbb{R} \tag{A.1}$$

Definition 7 (Derivative with respect to a vector)**.** We define the derivative of $F(x(\boldsymbol{w}))$ with respect to a vector $\boldsymbol{w}$ of p elements as the $M \times p$ matrix

$$\frac{\partial F}{\partial \boldsymbol{w}} \triangleq \begin{bmatrix} \frac{\partial f_1}{\partial \boldsymbol{w}_1} & \frac{\partial f_1}{\partial \boldsymbol{w}_2} & \cdots & \cdots & \frac{\partial f_1}{\partial \boldsymbol{w}_p} \\ \frac{\partial f_2}{\partial \boldsymbol{w}_1} & \frac{\partial f_2}{\partial \boldsymbol{w}_2} & \cdots & \cdots & \frac{\partial f_2}{\partial \boldsymbol{w}_p} \\ \vdots & \vdots & \vdots & \vdots & \vdots \\ \frac{\partial f_M}{\partial \boldsymbol{w}_1} & \frac{\partial f_M}{\partial \boldsymbol{w}_2} & \cdots & \cdots & \frac{\partial f_M}{\partial \boldsymbol{w}_p} \end{bmatrix} \tag{A.2}$$

Definition 8 (Derivative with respect to a matrix)**.** We define the derivative of $F(\boldsymbol{x}(W))$ with respect to a matrix W, being W_j the j^{th} column of a $p \times m$ matrix W as the $M \times (p \cdot m)$ matrix:

$$\frac{\partial F}{\partial W} \triangleq \left[\begin{array}{c|c|c|c} \frac{\partial F}{W_1} & \frac{\partial F}{W_2} & \cdots & \frac{\partial F}{W_m} \end{array} \right] \tag{A.3}$$

Please note that according to this definitions $\nabla f(x)$ with $f : \mathbb{R}^N \to \mathbb{R}$ corresponds to $\frac{\partial f}{\partial \boldsymbol{x}}^T$.

Definition 9 (Immediate derivative)**.** Consider a recurrence

$$a^k(\boldsymbol{x}) = F(\boldsymbol{x}(\boldsymbol{w})) + R(a^{k-1}(\boldsymbol{x}(\boldsymbol{w})), \ldots, a^0(\boldsymbol{x}(\boldsymbol{w})))$$

We define the immediate derivative of $a^k(\boldsymbol{x}(\boldsymbol{w}))$ with respect to the vector $\boldsymbol{w}$ the matrix

$$\frac{\partial^+ a^k}{\partial \boldsymbol{w}} \triangleq \frac{\partial F}{\partial \boldsymbol{w}}. \tag{A.4}$$

Appendix B

Details of the synthetic tasks

For the sake of completeness in this appendix we report all the details on the synthetic tasks we used as benchmarks in the present thesis. It should be noted that these tasks, amongst some similar other ones, have been introduced by Hochreiter [11] in 1991 and have been used as example of particularly difficult problem for RNNs to solve since.

These tasks are particularly difficult because they require learning long term correlations, i.e. memory and hence are perfect to test algorithms that should be able to deal with the vanishing gradient problem. A few additions are taken from Martens [19].

The addition problem The problem consists in performing an addition between two real numbers x_i and x_j in $[-1, 1]$ belonging to a sequence of randomly generated numbers. The difficulty in this problem is that such numbers can be arbitrarily distant in the input sequence, so the learning net must exhibit a long term memory. More specifically the input is a sequence of pairs; each pair is composed of a real number and a marker $\in \{1, 0\}$. The marker is used to select the two numbers in the sequence to add. The prediction is the last value in the output sequence, the target is $\frac{x_i+x_j}{2}$. The prediction y is considered correct if $|y - \frac{x_i+x_j}{2}| < 0.04$.

Sequences have random length, say L, between the minimal sequence length T and $T + \frac{T}{10}$, the position of the first marker is sampled in first $\frac{L}{10}$ positions, the last marker is instead sampled in $[\frac{4L}{10}, \frac{5L}{10}]$

The multiplication problem The problem is very similar to the addition problem, here we select two numbers in the input sequences of real numbers in $[0, 1]$ and we need to predict the product.

The XOR problem Again, the problem is the same as the addition one but the input are binary and we are asked to predict the XOR binary operation. This problem has been found particularly hard for both LSTM and hessian-free methods as reported in [19].

The temporal order problem The input sequences are composed of T randomly chosen symbols in $\{a, b, c, d\}$ except for two randomly selected positions for which the symbols are sampled in $\{x, y\}$. The task is to predict the relative order of the two special symbols, that is $\{xx, xy, yx, yy\}$. A variant of the task is to use three special symbols instead of two. Again, the difficulty of the problem is the possibly distance from the special symbols whose relative order is to be detected.

Bibliography

[1] Justin Bayer, Christian Osendorfer, Nutan Chen, Sebastian Urban, and Patrick van der Smagt. On fast dropout and its applicability to recurrent networks. *CoRR*, abs/1311.0701, 2013.

[2] Yoshua Bengio, Nicolas Boulanger-Lewandowski, and Razvan Pascanu. Advances in optimizing recurrent networks. In *IEEE International Conference on Acoustics, Speech and Signal Processing, ICASSP 2013, Vancouver, BC, Canada, May 26-31, 2013*, pages 8624–8628. IEEE, 2013.

[3] Yoshua Bengio, Jérôme Louradour, Ronan Collobert, and Jason Weston. Curriculum learning. In *Proceedings of the 26th Annual International Conference on Machine Learning*, ICML '09, pages 41–48, New York, NY, USA, 2009. ACM.

[4] Yoshua Bengio, Patrice Simard, and Paolo Frasconi. Learning long-term dependencies with gradient descent is difficult. *IEEE Transactions on Neural Networks*, 5(2):157–166, 1994.

[5] Nicolas Boulanger-Lewandowski, Yoshua Bengio, and Pascal Vincent. Modeling temporal dependencies in high-dimensional sequences: Application to polyphonic music generation and transcription. In *Proceedings of the 29th International Conference on Machine Learning, ICML 2012, Edinburgh, Scotland, UK, June 26 - July 1, 2012*. icml.cc / Omnipress, 2012.

[6] Kyunghyun Cho, Bart van Merrienboer, Çaglar Gülçehre, Dzmitry Bahdanau, Fethi Bougares, Holger Schwenk, and Yoshua Bengio. Learning phrase representations using RNN encoder-decoder for statistical machine translation. In *Proceedings of the 2014 Conference on Empirical Methods in Natural Language Processing, EMNLP 2014, October 25-29, 2014, Doha, Qatar, A meeting of SIGDAT, a Special Interest Group of the ACL*, pages 1724–1734, 2014.

[7] Junyoung Chung, Çaglar Gülçehre, KyungHyun Cho, and Yoshua Bengio. Empirical evaluation of gated recurrent neural networks on sequence modeling. *CoRR*, abs/1412.3555, 2014.

[8] Junyoung Chung, Çaglar Gülçehre, KyungHyun Cho, and Yoshua Bengio. Gated feedback recurrent neural networks. *CoRR*, abs/1502.02367, 2015.

[9] Tom Fawcett. An introduction to roc analysis. *Pattern Recognition Letters*, 27(8):861–874, June 2006.

[10] Alex Graves. Generating sequences with recurrent neural networks. *CoRR*, abs/1308.0850, 2013.

[11] Sepp Hochreiter and Jürgen Schmidhuber. Long short-term memory. *Neural Computation*, 9(8):1735–1780, November 1997.

[12] Kurt Hornik, Maxwell Stinchcombe, and Halbert White. Multilayer feedforward networks are universal approximators. *Neural Networks*, 2(5):359–366, July 1989.

[13] Heikki Hyötyniemi. Turing machines are recurrent neural networks. In J. Alander, T. Honkela, and Jakobsson M, editors, *STeP '96 - Genes, Nets and Symbols; Finnish Artificial Intelligence Conference, Vaasa 20-23 Aug. 1996*, pages 13–24, Vaasa, Finland, 1996. University of Vaasa, Finnish Artificial Intelligence Society (FAIS). STeP '96 - Genes, Nets and Symbols; Finnish Artificial Intelligence Conference, Vaasa, Finland, 20-23 August 1996.

[14] Herbert Jaeger, Mantas Lukosevicius, Dan Popovici, and Udo Siewert. Optimization and applications of echo state networks with leaky- integrator neurons. *Neural Networks*, 20(3):335–352, 2007.

[15] Rafal Józefowicz, Wojciech Zaremba, and Ilya Sutskever. An empirical exploration of recurrent network architectures. In Francis R. Bach and David M. Blei, editors, *Proceedings of the 32nd International Conference on Machine Learning, ICML 2015, Lille, France, 6-11 July 2015*, volume 37 of *JMLR Proceedings*, pages 2342–2350. JMLR.org, 2015.

[16] Mantas Lukosevicius and Herbert Jaeger. Reservoir computing approaches to recurrent neural network training. *Computer Science Review*, 3(3):127–149, 2009.

[17] Mantas Lukoševičius and Herbert Jaeger. Survey: Reservoir computing approaches to recurrent neural network training. *Computer Science Review*, 3(3):127–149, August 2009.

[18] Wolfgang Maass, Thomas Natschlaeger, and Henry Markram. Real-time computing without stable states: A new framework for neural computation based on perturbations. *Neural Computation*, 14(11):2531–2560, 2002.

[19] James Martens and Ilya Sutskever. Training deep and recurrent networks with hessian-free optimization. In Grégoire Montavon, Genevieve B. Orr, and Klaus-Robert Müller, editors, *Neural Networks: Tricks of the Trade - Second Edition*, volume 7700 of *Lecture Notes in Computer Science*, pages 479–535. Springer, 2012.

[20] Tomáš Mikolov. *Statistical Language Models Based on Neural Networks.* PhD thesis, 2012.

[21] Tomas Mikolov, Armand Joulin, Sumit Chopra, Michaël Mathieu, and Marc'Aurelio Ranzato. Learning longer memory in recurrent neural networks. *CoRR*, abs/1412.7753, 2014.

[22] Arkadi Nemirovski, Anatoli Juditsky, Guanghui Lan, and Alexander Shapiro. Robust stochastic approximation approach to stochastic programming. *SIAM Journal on Optimization*, 19(4):1574–1609, 2009.

[23] Yurii Nesterov. A method of solving a convex programming problem with convergence rate O(1/sqr(k)). *Soviet Mathematics Doklady*, 27:372–376, 1983.

[24] Razvan Pascanu, Tomas Mikolov, and Yoshua Bengio. Understanding the exploding gradient problem. *CoRR*, abs/1211.5063, 2012.

[25] Razvan Pascanu, Tomas Mikolov, and Yoshua Bengio. On the difficulty of training recurrent neural networks. In *Proceedings of the 30th International Conference on Machine Learning, ICML 2013, Atlanta, GA, USA, 16-21 June 2013*, pages 1310–1318, 2013.

[26] Boris T. Polyak. Some methods of speeding up the convergence of iteration methods. *USSR Computational Mathematics and Mathematical Physics*, 4(5):1 – 17, 1964.

[27] David E. Rumelhart, Geoffry E. Hinton, and Ronald J. Williams. Parallel distributed processing: Explorations in the microstructure of cognition, vol. 1. In David E. Rumelhart, James L. McClelland, and CORPORATE PDP Research Group, editors, *Parallel Distributed Processing: Explorations in the Microstructure of Cognition, Volume 1: Foundations*, chapter Learning Internal Representations by Error Propagation, pages 318–362. MIT Press, Cambridge, MA, USA, 1986.

[28] Franco Scarselli and Ah Chung Tsoi. Universal approximation using feedforward neural networks: A survey of some existing methods, and some new results. *Neural Networks*, 11(1):15–37, January 1998.

[29] Nicol N. Schraudolph. Fast curvature matrix-vector products for second-order gradient descent. *Neural Computation*, 14(7):1723–1738, 2002.

[30] Hava T. Siegelmann and Eduardo D. Sontag. Turing computability with neural nets. *Applied Mathematics Letters*, 4:77–80, 1991.

[31] Nitish Srivastava, Geoffrey E. Hinton, Alex Krizhevsky, Ilya Sutskever, and Ruslan Salakhutdinov. Dropout: a simple way to prevent neural networks from overfitting. *Journal of Machine Learning Research*, 15(1):1929–1958, 2014.

[32] Ilya Sutskever, James Martens, George E. Dahl, and Geoffrey E. Hinton. On the importance of initialization and momentum in deep learning. In *Proceedings of the 30th International Conference on Machine Learning, ICML 2013, Atlanta, GA, USA, 16-21 June 2013*, volume 28 of *JMLR Proceedings*, pages 1139–1147. JMLR.org, 2013.

[33] Ronald J. Williams and Jing Peng. An efficient gradient-based algorithm for on-line training of recurrent network trajectories. *Neural Computation*, 2:490–501, 1990.

[34] Wojciech Zaremba and Ilya Sutskever. Learning to execute. *CoRR*, abs/1410.4615, 2014.

[35] Wojciech Zaremba, Ilya Sutskever, and Oriol Vinyals. Recurrent neural network regularization. *CoRR*, abs/1409.2329, 2014.